

University of Memphis

University of Memphis Digital Commons

---

Electronic Theses and Dissertations

---

12-1-2011

## In Vitro Evaluation of Electrospun Chitosan Mats Crosslinked with Genipin as Guided Tissue Regeneration Barrier Membranes

Peter A. Norowski Jr.

Follow this and additional works at: <https://digitalcommons.memphis.edu/etd>

---

### Recommended Citation

Norowski, Peter A. Jr., "In Vitro Evaluation of Electrospun Chitosan Mats Crosslinked with Genipin as Guided Tissue Regeneration Barrier Membranes" (2011). *Electronic Theses and Dissertations*. 389. <https://digitalcommons.memphis.edu/etd/389>

This Dissertation is brought to you for free and open access by University of Memphis Digital Commons. It has been accepted for inclusion in Electronic Theses and Dissertations by an authorized administrator of University of Memphis Digital Commons. For more information, please contact [khhgerty@memphis.edu](mailto:khhgerty@memphis.edu).

*IN VITRO* EVALUATION OF ELECTROSPUN CHITOSAN MATS CROSSLINKED  
WITH GENIPIN AS GUIDED TISSUE REGENERATION BARRIER MEMBRANES

by

Peter Andrew Norowski Jr.

A Dissertation

Submitted in Partial Fulfillment of the

Requirements for the Degree of

Doctor of Philosophy

Major: Biomedical Engineering

The University of Memphis

December, 2011

## **DEDICATION**

This work is dedicated to my friends, family, mother, father, brothers and late step-father, Tom. Without their support, this work would not be possible. This work is dedicated to those who always supported me, and to those who have instilled in me a love of learning, science and hard-work. Thank you.

## ACKNOWLEDGMENTS

I would like to acknowledge my primary advisor Dr. Bumgardner, whose input and guidance has been instrumental in shaping my graduate experience. Dr. Haggard has been instrumental in giving the project direction and suggesting relevant testing methodologies. I would also like to thank Dr. Jegdish Babu, who helped me acquire anaerobic culture skills and performed the work with periodontal pathogens. Dr. Clem and Dr. Eckstein provided valuable insight into electrospinning and also help sculpt the breadth and depth of the analysis. Dr. Adatrow gave his valuable clinical insight. I would also like to thank Dr Ping Li who discussed inflammation with me, and Dr. Judith Cole who shaped my understanding of cell signaling. I would like to thank Dr. Omar Skalli for helping me troubleshoot problems with fixing and staining cells. I would also like to thank, my friend, Ms. Lou Boykins, who helped me with SEM imaging and image analysis. I would also like to thank Mr. Binod Raj and Dr. Mishra for helping me complete the XRD measurements.

This work was supported in part by grants from the Department of Defense, the University of Memphis Faculty Research Program and The Biomaterials Applications of Memphis (BAM) research labs at the Joint University of Memphis-University of Tennessee Health Science Center Biomedical Engineering Program, Memphis, TN.

## ABSTRACT

Norowski, Peter Andrew. Ph.D. The University of Memphis. December 2011. In Vitro Evaluation of Electrospun Chitosan Mats Crosslinked with Genipin as Guided Tissue Regeneration Barrier Membranes. Major Professor: Joel D. Bumgardner Ph.D.

Guided tissue regeneration (GTR) is a surgical technique commonly used to exclude bacteria and soft tissues from bone graft sites in oral/maxillofacial bone graft sites by using a barrier membrane to maintain the graft contour and space. Current clinical barrier membrane materials based on expanded polytetrafluoroethylene (ePTFE) and bovine type 1 collagen are non-ideal and experience a number of disadvantages including membrane exposure, bacterial colonization/biofilm formation and premature degradation, all of which result in increased surgical intervention and poor bone regeneration. These materials do not actively participate in tissue regeneration, however bioactive materials, such as chitosan, may provide advantages such as the ability to stimulate wound healing and de novo bone formation. Our hypothesis is that electrospun chitosan GTR membranes will support cell attachment and growth but prevent cell infiltration/penetration of membrane, demonstrate *in vitro* degradation predictive of 4-6 month *in vivo* functionality, and will deliver antibiotics locally to prevent/inhibit periopathogenic complications. To test this hypothesis a series of chitosan membranes were electrospun, in the presence or absence of genipin, a natural crosslinking agent, at concentrations of 5 and 10 mM. These membranes were characterized by scanning electron microscopy, tensile testing, suture pullout testing, Fourier transform infrared spectroscopy, X-ray diffraction, and gel permeation chromatography, and *in vitro* biodegradation for diameter/morphology of fibers, membrane strengths, degree of crosslinking, crystallinity, molecular weight, and degradation kinetics, respectively. Cytocompatibility of membranes was evaluated in osteoblastic, fibroblastic and monocyte

cultures. The activity of minocycline loaded and released from the membranes was determined in zone of inhibition tests using *P. gingivalis* microbe. The results demonstrated that genipin crosslinking extended the *in vitro* degradation timeframe, extended the release of minocycline, and increased the tensile strength of the resultant membranes while cytocompatibility, swelling, and tear strength were unaffected. In conclusion, electrospun chitosan membranes crosslinked with genipin are a suitable material for guided tissue regeneration and may help reduce bacterial infection and bacteria-induced host inflammatory response.

## PREFACE

The main body of the work presented in this dissertation is aimed at characterizing and evaluating the potential of genipin-crosslinked electrospun chitosan membranes to act as guided tissue regeneration membranes. The work was been organized and submitted to or prepared for submission to three peer-reviewed journals for publication. Chapter 2 is submitted and under consideration for publication in the Journal of Tissue Engineering and Regenerative Medicine as a manuscript entitled “Novel naturally crosslinked electrospun nano-fibrous chitosan mats for guided bone regeneration membranes: material characterization and cytocompatibility.” Chapter 3 is prepared for submission to the Journal of Biomedical Materials Research - Part A in a manuscript entitled “Suture pullout strength and *in vitro* fibroblast and RAW 264.7 monocyte biocompatibility of genipin crosslinked nano-fibrous chitosan mats for guided tissue regeneration.” Chapter 4 of this dissertation will be submitted for publication in the Journal of Journal of Antimicrobial Chemotherapy as a manuscript entitled “Antimicrobial activity of minocycline-loaded genipin-crosslinked electrospun chitosan membranes for guided tissue regeneration.”

## TABLE OF CONTENTS

Chapter	Page
List of Figures	ix
1. Introduction	1
Background	1
Hypothesis	9
2. Submission to JOURNAL OF TISSUE ENGINEERING AND REGENERATIVE MEDICINE Novel naturally crosslinked electrospun nano-fibrous chitosan mats for guided bone regeneration membranes: material characterization and cytocompatibility	10
2.1. Abstract	10
2.2. Introduction	11
2.3. Materials and Methods	14
2.4. Results	18
2.5. Discussion	23
2.6. Conclusion	28
2.7. References	29
3. Submission to JOURNAL OF BIOMEDICAL MATERIALS RESEARCH - PART A Suture pullout strength and <i>in vitro</i> fibroblast and RAW 264.7 monocyte biocompatibility of genipin crosslinked nano-fibrous chitosan mats for guided tissue regeneration.	32
3.1. Abstract	32
3.2. Introduction	33
3.3. Materials and Methods	36
3.4. Results	39
3.5. Discussion	45

Chapter	Page
3.6. Conclusion	49
3.7. References	50
4. Submission to JOURNAL OF ANTIMICROBIAL CHEMOTHERAPY Antimicrobial activity of minocycline-loaded genipin-crosslinked electrospun chitosan membranes for guided bone regeneration	54
4.1. Abstract	54
4.2. Introduction	55
4.3. Materials and Methods	58
4.4. Results	60
4.5. Discussion	62
4.6. Conclusion	63
4.7. References	64
5. CONCLUSIONS	67
6. RECOMMENDATIONS	70
7. REFERENCES	73

## LIST OF FIGURES

Figure	Page
Figure 1.1 – Side view of electrospinning apparatus	8
Figure 1.2 – View of the electrospinning collection target	8
Figure 2.1 – Representative SEM images	19
Figure 2.2 – <i>In vitro</i> Biodegradation	20
Figure 2.3 – Ultimate tensile strength	20
Figure 2.4 – Fourier Transform Infrared Spectroscopy	21
Figure 2.5 – 5 day growth study of SAOS-2 osteoblastic cells	22
Figure 2.6 – Live-dead <sup>TM</sup> images of SAOS-2 cells on electrospun membranes	22
Figure 3.1 – Suture pullout testing setup	41
Figure 3.2 – Membrane specimens after suture pullout	41
Figure 3.3 – Ultimate pullout load normalized to membrane thickness	42
Figure 3.4 – <i>In vitro</i> cytocompatibility with NhDF fibroblasts	43
Figure 3.5 – NO production from RAW 264.7 in the presence of 0 µg/mL LPS	43
Figure 3.6 – NO production from RAW 264.7 in the presence of 1 µg/mL LPS	44
Figure 3.7 – Viability of RAW 264.7 at day 3.	44
Figure 4.1 – Swelling of electrospun chitosan mats in PBS	60
Figure 4.2 – Inhibition of <i>P. gingivalis</i> from mats with 10 mg/mL minocycline	61
Figure 4.3 – Inhibition of <i>P. gingivalis</i> from mats with 5 mg/mL minocycline	61

## **Chapter 1. Introduction**

### **Background**

Guided bone regeneration (GBR) and guided tissue regeneration (GTR) are conceptually similar: the prior is concerned with the formation of bone, and the latter is a wider term used to describe the guided regeneration of bone and/or associated soft tissues. These surgical procedures use an implant known as a barrier membrane, to maintain the contour and space by excluding the faster healing soft tissue from the bone graft space. Barrier membranes are used in many surgical applications. They are commonly used to maintain the space of any significantly large bone graft placed in the craniofacial regions, and along with bleeding bone and graft material help maintain a localized osteogenic environment [1]. Procedures that may require the use of a barrier membrane include bone grafts due to bone resection, bone atrophy [2] or trauma [3], socket preservation [1], orbital floor reconstruction [4], osteotomy and cleft palate repair [5], sinus augmentation (to repair a perforated sinus membrane) [6], and also compound distal tibial fractures and other challenging orthopedic reconstructions [7, 8].

However, one of the most heavily researched and challenging applications of barrier membranes is when they are used to treat intra-bony defects associated with periodontitis [1, 3, 9-21]. Periodontitis is an inflammatory disease that causes the destruction of supporting bone and soft tissue around teeth. It is reported that 31% of people in the United States display mild forms, 13% show moderate severity, and 4% have advanced disease symptoms [22]. As much as 40-50% of the worldwide adult population exhibits some form of periodontitis [23]. This inflammatory disease, driven by gram negative bacteria, termed periopathogens, causes the host-mediated destruction

of soft tissue and bone eventually leading to the premature loss of the tooth [24]. The tissue destruction is localized around the supporting tissues of a tooth creating a periodontal lesion, or an intra-bony defect with a deep gingival pocket where anaerobic gram-negative bacteria can thrive. There are a variety of periodontal treatment options that can be undertaken to save a tooth suffering from periodontitis, but for periodontal pockets deeper than 4.2 mm, surgical treatment is advocated to restore bony height and clinical attachment [25, 26]. Research has shown that use of GTR barrier membranes to treat periodontal defects improves clinical parameters, including soft tissue attachment gain and hard tissue gain, compared to open flap debridement surgery alone [15]. However, the improvements in clinical outcome are widely variable and unpredictable when using GTR membranes [15]. Even more clinically challenging is restoring bone in patients who are smokers, diabetics [27], or when the defect is large and deep enough to involve the furcation of the tooth [18-21]. The mechanism of action of barrier membranes is thought to be that they exclude the faster healing soft tissues of the gingiva and support a localized osteogenic environment in the graft space. There are a multitude of bone graft products which generate bone quite predictably, but the remaining clinical challenge is regeneration of associated soft tissues of the tooth, specifically the periodontal ligament and cementum (where the ligament anchors into the root surface).

Clinically-used barrier membrane materials include expanded polytetrafluoroethylene (ePTFE), degradable synthetic polymers, and bovine type 1 collagen. The consensus is that in terms of bone regeneration capabilities, i.e. the ability to restore bony height (clinical attachment level), ePTFE membranes are the gold standard, followed by type 1 collagen membranes, and synthetic polymers are a distant

third and are not used as often [28-30]. However, many clinicians prefer collagen membranes to ePTFE because they are easier to handle and do not require a follow-up membrane-removal surgery, which is time-consuming, costly, and painful to the patient. Collagen membranes have their own set of drawback including rapid and unpredictable degradation, and they may not maintain barrier function for the full healing and regeneration period of 4-6 months [31]. Collagen membranes, crosslinked with glutaraldehyde, have slower degradation rates, but they also have poor tissue response, become exposed more often [32] and elicit less bone formation than uncrosslinked collagen membranes [31]. Additional problems with collagen and ePTFE membranes include infection, wound dehiscence and membrane exposure [14, 33, 34] and premature membrane degradation [31] especially when exposed to the oral cavity [32]. Synthetic polymer membranes are typically composed of poly-lactide-co-glycolide and are associated with lower bone volumes, poor tissue healing response, acidic degradation products, and membrane exposure [35-40].

The problem with current GTR therapies for surgical treatment of periodontitis, is that they are intended to restore the anatomical defect, but do not address the underlying etiology of the disease. That is why for patients with chronic or unresolved periodontitis, standard periodontal treatment is advocated before GTR or GBR therapy can begin [41]. This is costly and time-consuming for both the patient and physician. A better approach would be to have a bioactive GTR material that can inhibit bacteria-induced sustained host-inflammatory response during tissue healing and maturation. This expanded function of the barrier membrane is a thin line to walk, because the transient expression of inflammatory cytokines is absolutely necessary for bone healing and remodeling.

However, sustained inflammation has been associated with a reduced bone formation [42].

The sequence of cell signaling events that occur during periodontal tissue destruction have been studied in depth [24, 43]. Lipopolysaccharide (LPS), which is the primary component of gram-negative bacteria outer cell walls, is the major driver of inflammatory cell recruitment and activation [24, 44]. Monocytes and activated macrophages are stimulated by LPS to express nitric oxide (NO), interleukin-1 $\beta$  (IL-1 $\beta$ ), tumor necrosis factor- $\alpha$  (TNF-  $\alpha$ ), among a myriad of other pro-inflammatory cytokines, which then recruit other cells to carry out tissue or bone breakdown. The primary culprits in the breakdown of collagen and surrounding tissues are collagenase and matrix metalloproteinases (MMPs) secreted by fibroblasts and polymorphonuclear leukocytes (PMNs). Osteoclasts are also recruited for the breakdown bone in the presence of receptor activator of nuclear factor-kappa B ligand (RANKL). Therapeutic approaches which simply eliminate pathogenic bacteria are temporary ameliorations at best, since after treatment has ended bacterial microflora can return. Furthermore, simple local administration of antibiotic has shown no clinical benefit to patients undergoing GTR procedures [45]. Next generation strategies involve the modulation of host-mediated inflammatory response. Therapies which inhibit the release of pro-inflammatory cytokines, or which inhibit the activation/differentiation of the involved the cell types, are thought to be of benefit to patients with periodontitis [24]. Additionally, elevated expression of NO in gingival and peri-apical tissues of patients with periodontitis has been reported in several studies [23, 46]. These findings demonstrates that pathogenesis of tissue destruction associated with periododntitis is, at least in part, dependent on NO

signaling pathways. While systemic inhibition of NO signaling or iNOS expression is clinically questionable, inhibition of NO in the periodontal tissues does appear to be a valid target for the inhibition of periodontitis associated tissue destruction [23, 46].

Chitosan is a promising biomaterial for application as a GTR membrane because it provides beneficial properties including increased bone formation and accelerated wound healing [47]. Chitosan is the deacetylated form of the biopolymer chitin, which possesses osteogenic properties [47, 48]. Chitosan's chemical structure is N-acetylglucosamine-co-N-glucosamine copolymer, that is more than 50% deacetylated. It can be manipulated into a variety of constructs including films, beads, scaffolds, coatings, fibers and nanofibers. Chitosan materials are derived from chitin, a biopolymer found in crustaceans or some fungi. The biological properties and degradation rate of chitosan materials can vary greatly by manipulating the degree of deacetylation (DDA), molecular weight, and crystallinity of the polymer. Chitosan and its degradation products (glucosamine sugars) are cytocompatible and non-acidic, unlike the degradation products associated with synthetic polymers.

For use as GTR barrier membranes Kuo et al. investigated chitosan films gelled with NaOH, and films crosslinked with  $\text{Na}_5\text{P}_3\text{O}_{10}$  and  $\text{Na}_2\text{SO}_3$  and demonstrated the ability to stimulate 21-31% more bone formation in rat calvaria than empty defect [49]. Films gelled with NaOH showed the greatest *de novo* bone formation [49]. Yeo et al. evaluated chitosan wet-spun non-woven membranes (100  $\mu\text{m}$  fiber) in canine one-wall intrabony mandibular defects [50]. They reported that chitosan non-woven meshes regenerated larger amounts of bone than biodegradable collagen membranes (Biomesh®, Samyang Co) while having comparable soft tissue attachment and barrier function.

Results at 8 weeks demonstrated that 42% of the bone height was restored by chitosan membranes as opposed to 32% and 26% for collagen membrane and control (no membrane), respectively. The wet-spinning and crosslinked film approaches demonstrated promising results, but nanofabricated chitosan membranes would offer additional benefits of permeability to nutrients and wastes, cell occlusion and biomimetic scale for tissue integration [51-53], while maintaining the inherent beneficial properties of chitosan biomaterials.

Materials can be fabricated into nano-fibrous constructs using a variety of techniques including self assembly, phase separation and sugar leaching, and electrospinning [54-59]. Electrospinning is a relatively inexpensive, simple, and reliable method for the manufacture of polymer nanofibers, and can result in random fiber orientation or highly aligned fiber orientation. The process works by using a large voltage potential (typically 10-30 kV) to electrostatically charge a polymer solution [58]. This electrostatic charge causes chain repulsion forces within the polymer solution which overcome the surface tension forces of that solution [58]. The result is a polymer fiber which is extruded from the charged solution and sent into flight toward the collection target. The collection target could be anything that is electrically grounded, including flat plates, spinning drums, coagulation solutions, scaffold or implant materials, or even a human hand. As the extruded fiber is driven toward the target, solvent evaporation and fiber elongation result in solidified polymer fibers which have diameters typically < 150 nm [60].

Using electrospinning techniques, researchers have been able to make nanofibrous constructs from synthetic polymers which regenerated dense cortical bone in rabbit tibia

[61]. Shin et al. used electrospinning to fabricate chitosan biopolymer nanofibrous GBR membranes to be biomimetic and provide cell occlusion [62]. They demonstrated that the electrospun chitosan membranes facilitated more new bone formation in critical size bone defects than control (empty defect) after 4 weeks in rabbit calvaria [62]. However, they noted that their electrospun chitosan membranes fragmented after 8 weeks of implantation in rat subcutaneous tissue. These studies demonstrated the potential of degradable chitosan membranes to maintain graft space and regenerate bone with minimal inflammatory response [49, 50, 62] but additional work on electrospun chitosan membranes is needed to improve the clinical handle-ability, strength, and degradation timeframe. In an effort to increase the strength and lengthen the degradation timeframe of electrospun chitosan membranes, Schiffmann and Schauer used glutaraldehyde to crosslink chitosan nanofibers [63, 64]. However, the glutaraldehyde crosslinking caused an increase in the average fiber diameter, did not increase the ultimate tensile strength of their chitosan membranes. Finally, they did not evaluate degradation or biocompatibility of the resultant mats.

The ideal GTR material should be easy to handle and manipulate, have sufficient strength to maintain the space of the graft site and to withstand suture or pin placement, be cell occlusive, allow for the diffusion of nutrients and wastes, and degrade on a timescale consistent with tissue healing and maturation. To meet these criteria, non-woven chitosan mats were made by electrospinning using a slowly rotating circular target to ensure random fiber orientation, and crosslinked using 5 mM or 10 mM genipin, a natural crosslinking agent isolated from the fruit of the gardenia plant (Figures 1.1 and 1.2).

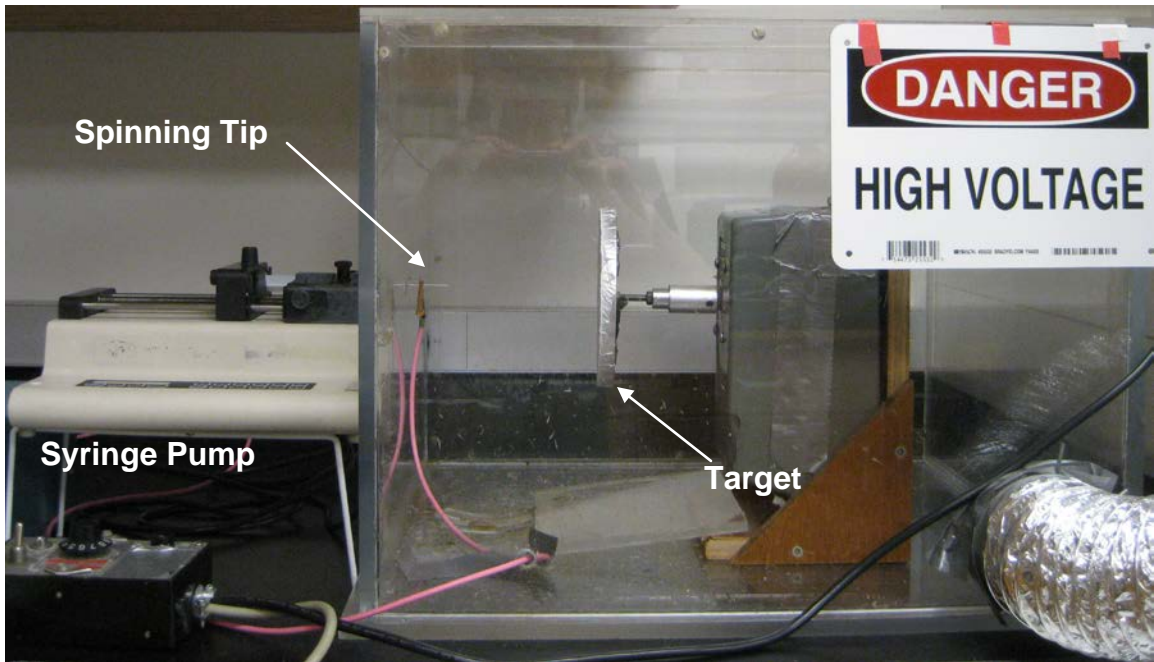


**Figure 1.1 - Side view of the electrospinning setup for fabricating genipin-crosslinked nano-fibrous chitosan mats.**



**Figure 1.2 – View of the collection target with nano-fibrous chitosan accumulation.**

## **Hypothesis**

The use of a biodegradable, nano-fibrous, bioactive, antimicrobial, chitosan mats strengthened by genipin crosslinking will result in improved clinical outcomes compared to current GTR membrane therapies by stimulating healing, reducing pathogenic bacteria, and reducing host mediated inflammation. Specifically, genipin-crosslinked electrospun chitosan should exhibit evidence of chemical crosslinking and should have a higher tensile and suture pullout strength than uncrosslinked membranes. Genipin-crosslinked electrospun chitosan membranes should degrade on a timescale consistent with tissue healing and bone maturation. Electrospun chitosan mats should not exhibit cytotoxic effects to osteoblasts, fibroblasts, or monocyte cells. Genipin-crosslinked electrospun membranes should maintain the capacity to deliver antibiotics or growth factors to the graft site as compared to uncrosslinked membranes. Finally, genipin-crosslinked electrospun chitosan membranes should be able to reduce LPS-induced monocyte activation in a manner similar to uncrosslinked membranes.

## **CHAPTER 2. Journal submission to the Journal of Tissue Engineering and Regenerative Medicine**

### **Novel naturally crosslinked electrospun nano-fibrous chitosan mats for guided bone regeneration membranes: material characterization and cytocompatibility.**

Authors: Peter A. Norowski Jr, Tomoko Fujiwara, William C. Clem, Pradeep C. Adatrow, Eugene C. Eckstein, Warren O. Haggard, Joel D. Bumgardner.

**Abstract:** Guided bone regeneration (GBR) barrier membranes are used to prevent soft tissue infiltration into the graft space during dental procedures that involve bone grafting. Chitosan materials have shown promise as GBR barrier membranes due to their biocompatibility and predictable biodegradability, but degradation rates may still be too high for clinical applications. In this study, chitosan GBR membranes were electrospun using chitosan (70% deacetylated, 312 kDa, 5.5 w/v%) with or without the addition of 5 or 10 mM genipin, a natural crosslinking agent, in order to extend the degradation to meet the clinical target timeframe of 4-6 months. Membranes were evaluated for fiber diameter, tensile strength, biodegradation rate, bond structure, and cytocompatibility. Genipin addition, at 5 or 10 mM, slightly reduced the fiber diameter from 165-228 nm for uncrosslinked to 142-197 nm. Crosslinking, examined by Fourier transform infrared spectroscopy, showed a decrease in N-H stretch as genipin levels were increased. Genipin-crosslinked mats exhibited only 22% degradation based on mass loss as compared to 34% for uncrosslinked mats at 16 weeks *in vitro*. The ultimate tensile strength of the mats was increased by 165% to 32 MPa with 10 mM crosslinking as compared to uncrosslinked mats. Finally, genipin-crosslinked mats supported the proliferation of SAOS-2 cells in a 5 day growth study, similar to uncrosslinked mats. Results suggest that electrospun chitosan mats may benefit from genipin crosslinking and have the potential to meet clinical degradation timeframes for GBR applications.

## 1. Introduction

In dental applications, guided bone regeneration (GBR) is a surgical technique used to direct the formation of bone during augmentation procedures where a barrier membrane is used to exclude the soft tissues from the bone graft space. Current clinically used membranes made from expanded polytetrafluoroethylene (ePTFE), a non-degradable woven material, require a second surgery for removal and are reported to have exposure/infection rates as high as 20-44% [1, 2]. The removal surgery may disrupt healing in the graft area and is a financial and physical burden to both the patient and physician. For this reason, many clinicians have begun to use degradable membranes which do not require removal [3]. Commercially available biodegradable membranes are typically made from porcine or bovine collagen. However, the degradation of these collagen materials is rapid and unpredictable and they may not maintain barrier function for the full healing and regeneration period of 4-6 months [4]. Collagen membranes, crosslinked with glutaraldehyde, have slower degradation rates, but they also have poor tissue response, become exposed more often [5] and elicit less bone formation than uncrosslinked collagen membranes [4]. Additional problems with collagen and ePTFE membranes include infection, wound dehiscence and membrane exposure [3, 6, 7] and premature membrane degradation [4] especially when exposed to the oral cavity [5].

Chitosan is a linear biopolymer composed of more than 50% N-glucosamine units in a N-acetyl-glucosamine –co- N-glucosamine copolymer. Chitosan materials have shown great potential in GBR applications because of their biocompatibility, controllable degradation, and non-toxic degradation products [8-10] and have been manufactured into fibers and sheets using a variety of techniques including electrospinning, wet-spinning,

and solution casting [8-13]. Electrospinning, which uses a high voltage source to manufacture polymer fibers, is well suited for the production of fibrous membranes because it is relatively cheap, simple, and can reliably reproduce fibers in the nano-range. Nano-fibrous membranes are particularly advantageous because they allow fluid and nutrient exchange through the membrane, mimic the topology of the extracellular matrix, and are cell occlusive. The extruded polymer fibers, which solidify as they are collected on the electrically grounded target, are deposited in random fashion until they collect into a non-woven randomly oriented fiber mat. This process yields pores that are too small to allow cellular infiltration.

Chitosan may be electrospun using specific solvents such as 1,1,1,3,3,3-hexafluoroisopropyl alcohol (HFIP) or trifluoroacetic acid (TFA) or is spun using copolymer mixtures with polyethylene oxide (PEO), polyvinyl alcohol (PVA), or collagen [14]. Typically electrospun fibers have a mean diameter of  $\leq 100$  nm, but can vary widely with diameters as large as 1  $\mu\text{m}$ , depending upon a number of factors such as polymer wt.%, polymer molecular weight, viscosity, voltage, temperature, and solvent properties such as surface tension to name a few [15].

Kuo et al. investigated chitosan films gelled with NaOH, and films crosslinked with  $\text{Na}_5\text{P}_3\text{O}_{10}$  and  $\text{Na}_2\text{SO}_3$  for use as GBR membranes and demonstrated good mechanical properties and were able to stimulate the formation of bone in rat calvaria better than controls (empty defect) [8]. Yeo et al. evaluated chitosan wet-spun non-woven membranes (100  $\mu\text{m}$  fiber) in canine one-wall intrabony mandibular defects [10]. They reported that chitosan non-woven meshes regenerated larger amounts of bone than biodegradable collagen membranes (Biomesh®, Samyang Co) while having comparable

soft tissue attachment and barrier function, and that, at 8 weeks, 42% of the bone height was restored by chitosan membranes as opposed to 32% and 26% for collagen membrane and control (no membrane), respectively. Though these results were promising, the wet-spinning approach did not offer all of the advantages of nanofabricated membranes such as cell occlusion and biomimetic scale. Using electrospinning techniques, Shin et al. made nanofibrous GBR membranes to be biomimetic and provide cell occlusion [9]. They demonstrated that the electrospun chitosan membranes facilitated more new bone formation in critical size bone defects than control (empty defect) after 4 weeks in rabbit calvaria [9]. However, they noted that their electrospun chitosan membranes fragmented after 8 weeks of implantation in rat subcutaneous tissue. These studies demonstrated the potential of degradable chitosan membranes to maintain graft space and regenerate bone with minimal inflammatory response [8-10] but additional work is needed to improve the clinical handle-ability, strength, and degradation timeframe of electrospun chitosan membranes.

In an effort to increase the strength and degradation timeframe of electrospun chitosan membranes, Schiffmann and Schauer used glutaraldehyde to crosslink chitosan nanofibers [12, 13]. However, the glutaraldehyde crosslinking caused an increase in the average fiber diameter, did not increase the ultimate tensile strength of their chitosan membranes, nor did they evaluate degradation or biocompatibility of the mats.

In this study, the natural crosslinker genipin, which is isolated from the fruit of the gardenia plant, was used to crosslink chitosan nanofibrous mats. Studies have shown that chitosan and gelatin membranes were more biocompatible, less inflammatory, and resulted in faster healing times when crosslinked with genipin instead of glutaraldehyde

[16-18]. Our goal was to extend the degradation of the chitosan membrane to the clinician suggested period of 4-6 months. Our hypothesis is that genipin-crosslinked chitosan mats will exhibit improved mechanical strength, extended degradation timeframe, and little or no cytotoxicity when compared to uncrosslinked chitosan mats.

## **2. Materials and Methods**

### **2.1 Electrospinning procedure**

To make electrospun chitosan nanofibrous mats a 5.50wt% chitosan solution in 70% trifluoroacetic acid and 30% methylene chloride was gently mixed overnight. Genipin is mixed into the polymer solution 30 minutes prior to the start of electrospinning at a concentration of 0, 5, or 10 mM. The solution was loaded into a plastic 10 mL syringe with a blunt 20G, 3.81 cm stainless steel needle tip. The syringe was loaded into a syringe pump and the flowrate set to 20  $\mu\text{L}/\text{min}$ . The solution was electrospun at 25 kV and the fibers were collected on a non-stick aluminum foil target (38.1 cm diameter disc), positioned 15 cm from needle tip and rotated at 8.4 rpm by an AC motor to ensure even and random distribution of fibers. The electrospinning apparatus was housed inside of a ventilated box, which was vented to the fume hood. After electrospinning, the nanofibrous mat was put under vacuum overnight to remove residual solvent, removed from the foil, and then neutralized in room temperature 5M  $\text{Na}_2\text{CO}_3$  (saturated solution) for 3 hours [11]. The membrane was then rinsed with deionized water until neutral. After drying at ambient conditions, mats were sterilized using ethylene oxide gas.

## **2.2 Scanning electron microscopy (SEM)**

SEM was used to view the morphology and determine the diameter of the electrospun fibers from two different mats of each type. To view fibers, representative 1 cm<sup>2</sup> samples were cut and then coated with 10 nm of gold-palladium to aid in imaging and reduce charging. All images were collected using Philips XL 30 ESEM (FEI Co., Hillsboro, OR). Fiber size was determined from 4 locations and viewed at 5000X for each sample and measuring diameters standard image analysis techniques.

## **2.3 Mechanical Testing.**

Mechanical testing was performed to determine ultimate tensile strength of the electrospun mats as an indicator of clinical handle-ability. Dog bone shaped specimens were cut from mats using a custom punch. The dimensions of the gauge length of the dog bone specimen were measured with digital caliper and were approximately 13x3.7x0.12 mm. Tensile testing (n=4) of dry dog-bone specimens was carried out using an Instron<sup>TM</sup> model 4465 mechanical test frame (Norwood, MA, USA) with a 500 N load cell and an extension rate of 1 mm/min.

## **2.4 Fourier Transform Infrared Spectroscopy (FTIR)**

In order to assess the level of crosslinking that occurred we examined the bond structure of the chitosan membranes by attenuated total reflectance FTIR. Spectra were collected from neutralized membrane samples (1 cm<sup>2</sup>; n=4) on a Nicolet FTIR spectrometer in absorbance mode. Membranes and background were scanned 64 times with a resolution of 4 cm<sup>-1</sup> according to ASTM F2103-01 (2009).

## **2.5 In vitro biodegradation**

To determine degradation profile of crosslinked and uncrosslinked electrospun membranes, samples 3 cm<sup>2</sup> in size were incubated at 37 °C in PBS containing 100 µg/mL lysozyme, supplemented with 500 I.U./mL penicillin, 500 µg/mL streptomycin, and 25 µg/mL amphotericin-B and the change in mass was recorded at 1, 2, 3, 4 and 16 weeks. This study was performed in PBS containing 100µg/mL lysozyme, a level much higher than physiological conditions. A high level of lysozyme was used in this study to accelerate degradation and differentiate any possible differences in biodegradation caused by crosslinking of the chitosan polymer. It was not intended to be predictive of clinical performance. Results are presented as the mass fraction remaining. Separate independent samples of 4 membranes per group were taken at each timepoint.

## **2.6 In vitro cell viability and proliferation.**

SAOS-2 human (Cat. No. HTB-85, ATCC, Manassas, VA, USA) osteoblastic cells were seeded on uncrosslinked and crosslinked nanofibrous membranes mounted in 24-well size CellCrown™ culture inserts (Scaffdex, Tampere, Finland). CellCrown™ inserts were used to keep membranes from floating in culture wells. Membranes were rinsed in culture media 4 times and then seeded at 1x10<sup>4</sup> cells per membrane. Cells were also seeded onto 24-well tissue culture plastic as a positive control. Cells were grown in McCoy's 5a medium supplemented with 10% FBS and 500 I.U./mL penicillin, 500 µg/mL streptomycin, and 25 µg/mL amphotericin-B. Proliferation was measured at days 1, 3, and 5 (n=4 per group per time point) using Cell Titre Glo™ luminescent cell viability assay (Promega, Madison, WI, USA). The assay measures the amount of light produced based on the oxidation of ATP, which is proportional to the total number of

cells, in the luciferin-luciferase reaction. Cell number was determined by means of a standard curve of SAOS-2 cells ranging from  $5 \times 10^3$  to  $2 \times 10^5$  cells/well seeded on tissue culture plastic twelve hours before assay. Cell viability and morphology was also observed by fluorescent microscopy using Live-Dead® stain (Molecular Probes, Eugene OR, USA). Images of cells growing on membranes were obtained by fluorescent microscopy (Nikon Eclipse TE300, Tokyo, Japan).

Statistically significant differences were detected by ANOVA followed by Student-Neuman-Kools (SNK) post-hoc test to determine where differences existed between groups. Statistical significance was declared at  $p < 0.05$ .

### 3. Results

Electrospun mats had a mean fiber diameter in the nano-range. Representative images are shown in Figure 1 and the fiber diameter from each of the 2 mats per group is summarized in Table 1. In general, genipin addition to the electrospinning solution resulted in smaller diameter fibers as compared to chitosan fibers electrospun without genipin.

The results of the degradation study are shown in Figure 2. Statistical analyses showed that there was a significant change in mass for all mats over time ( $p < 0.05$ ) and between groups ( $p < 0.05$ ). Uncrosslinked chitosan mats resulted in the greatest loss in mass and 10 mM genipin crosslinked mats resulted in the least loss. While significant differences may not exist between all groups at each time point, at 16 weeks (4 months), uncrosslinked mats had lost (34%) significantly more mass than 10 mM crosslinked mats (22%), while 5 mM (28%) was not significantly different from either.

Mechanical testing revealed that the tensile strength is significantly increased upon crosslinking with genipin (Figure 3). The ultimate tensile strength was  $12.3 \pm 5.0$  MPa for uncrosslinked chitosan mats, which increased to  $22.2 \pm 6.8$  and  $32.2 \pm 8.1$  MPa for crosslinking with 5 and 10 mM genipin, respectively.

Representative FTIR spectra of the uncrosslinked mat and of each level of genipin crosslinked chitosan mats are shown in Figure 4. FTIR spectra gathered from all groups of electrospun mats exhibited amide I ( $1651 \text{ cm}^{-1}$ ), amide II ( $1586 \text{ cm}^{-1}$ ), amide III ( $1321 \text{ cm}^{-1}$ ) and C-O-C ( $1032, 1082, 1152 \text{ cm}^{-1}$ ) peaks typical of chitosan structure. The N-H stretch peak is found at  $3372 \text{ cm}^{-1}$  atop the larger and more broad O-H stretch peak and is interpreted as the free amino groups present on the chitosan polymer. The height of the

N-H stretch peak decreased by 60% and 86% for chitosan mats electrospun with 5 mM and 10 mM genipin, respectively.

There were no statistical differences in the 5 day growth of cells on crosslinked membranes as compared to uncrosslinked membranes (Figure 5). Osteoblastic cells on all membrane types were viable and had a low proportion of non-viable cells as shown by Live-Dead® stain (Figure 6). No differences in morphology or viability of the cells, based on visual inspection, on the membranes were observed.

**Table 1 – Fiber diameters  $\pm$  standard deviation of electrospun chitosan mats as measured via image analysis at 5000X magnification.**

	Mat 1 fiber diameter (nm)	Mat 2 fiber diameter (nm)
Uncrosslinked	162 $\pm$ 98	228 $\pm$ 116
5 mM genipin	142 $\pm$ 90	160 $\pm$ 61
10 mM genipin	142 $\pm$ 56	197 $\pm$ 68

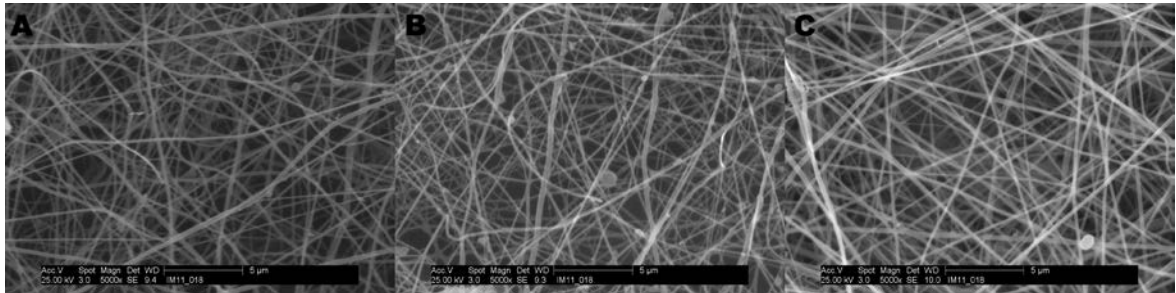


**Figure 1 – representative SEM images of A) uncrosslinked, B) 5 mM genipin crosslinked and C) 10 mM genipin crosslinked chitosan fibers.**

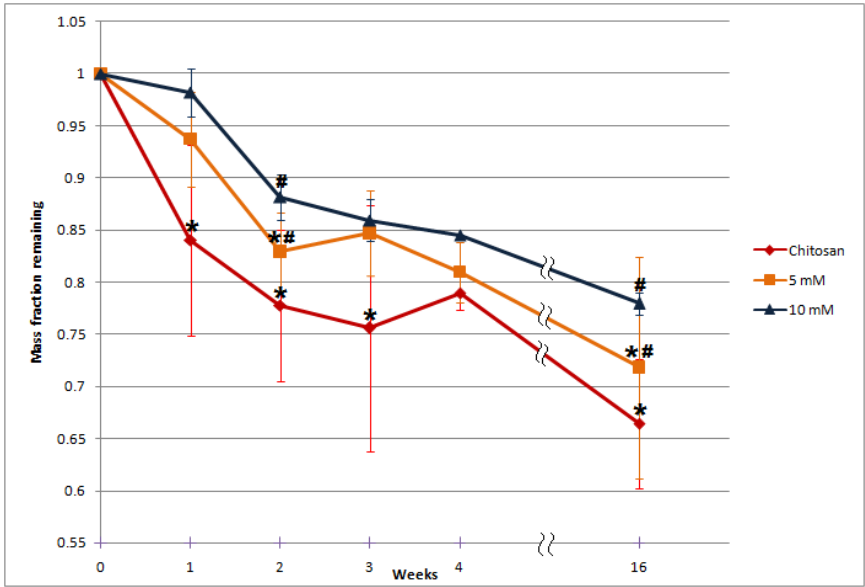


**Figure 2 – *In vitro* biodegradation measured by mass loss over a 16 weeks in PBS+100 µg/mL lysozyme at 37°C. The mass fraction remaining is plotted against time in weeks. The \* and # denote statistical significance (p<0.05) as determined by ANOVA and SNK post-hoc test.**

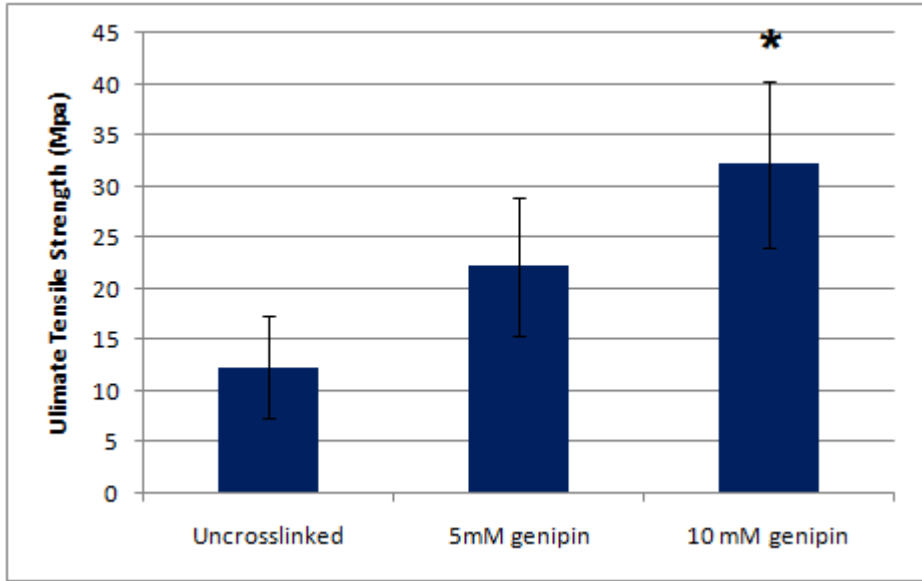


**Figure 3 – Ultimate tensile strength of the dry electrospun membranes (n=4) \* indicates significant difference p<0.05.**

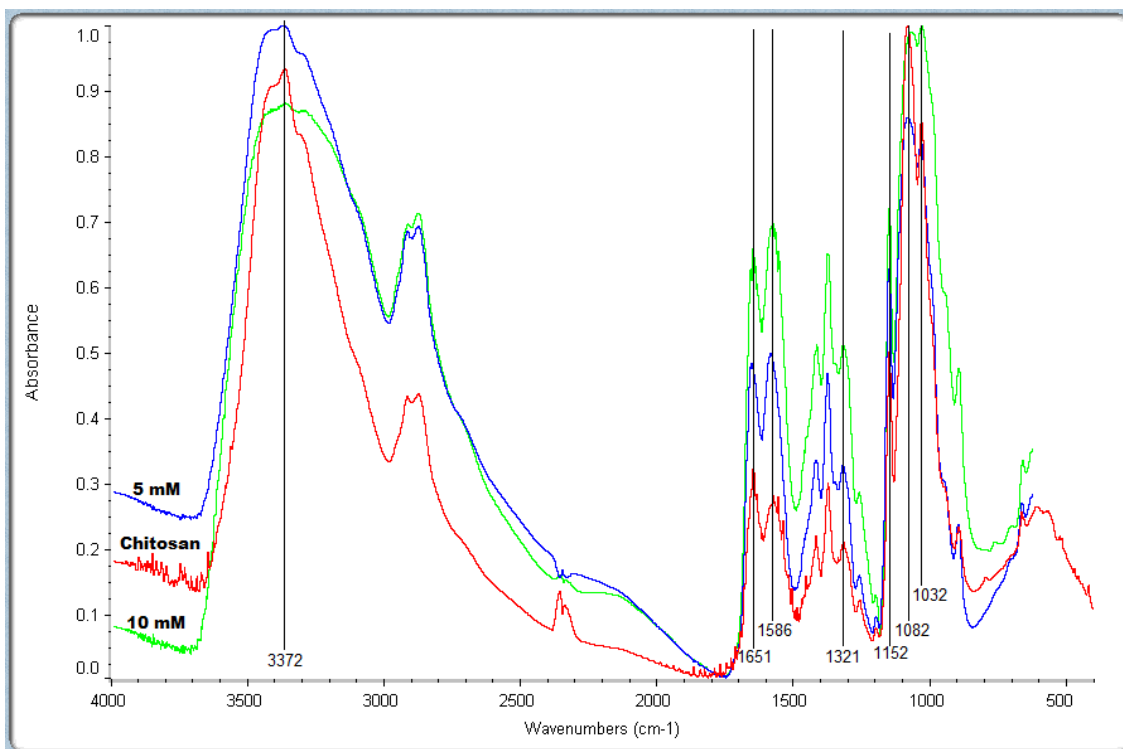


**Figure 4 – FTIR spectra from uncrosslinked chitosan (red), 5 mM crosslinked chitosan (blue) and 10 mM crosslinked chitosan (green). Note the diminishing N-H stretch peak at 3372 cm<sup>-1</sup>, which is the narrow peak atop the larger O-H stretch peak. With higher levels of crosslinking the free amino peak is decreasing indicating that the genipin is crosslinking at that site. Other labeled peaks are associated with the glucosamine structure of chitosan.**

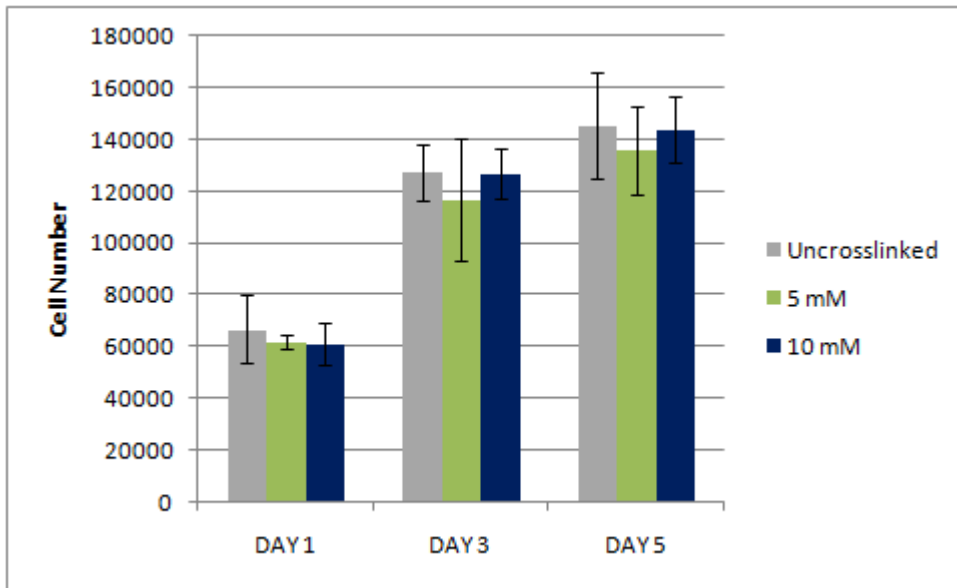


**Figure 5 – The number of SAOS cells present on the membrane after 1-5 days of culture determined by a standard curve of cell densities seeded 12 hours before reading. No significant difference were found (n=4).**

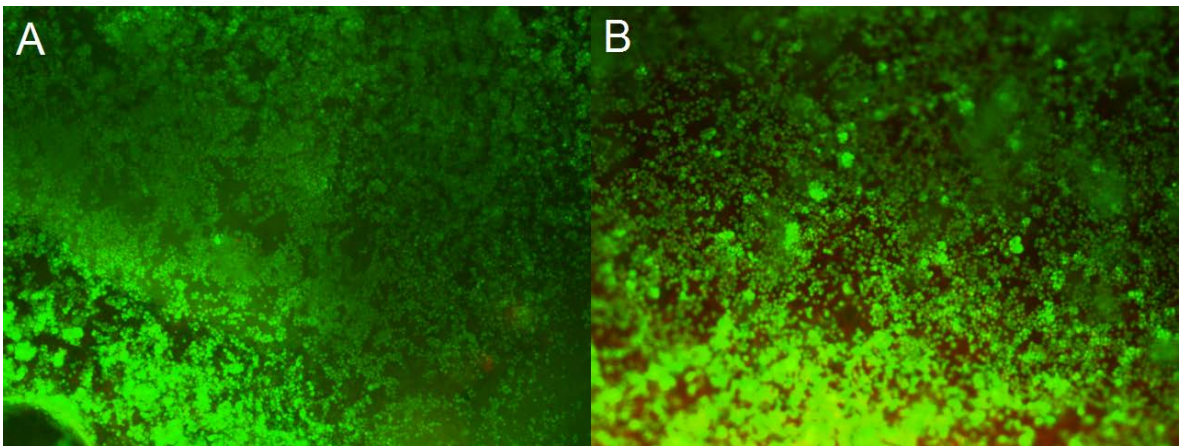


**Figure 6: Live dead stain of SAOS-2 cells on day 5 at 40X magnification. A) Uncrosslinked chitosan B) 10 mM genipin crosslinked. Note the large number of green viable cells. Results were similar for 5 mM (not shown).**

#### **4. Discussion**

Chitosan has shown promise as a GBR membrane material, but degradation has not been optimized to maintain effective barrier function for the target 4-6 months of healing. In this study, we investigated the hypothesis that genipin crosslinking of electrospun chitosan would improve mechanical properties, prolong degradation timeframe, and exhibit cytocompatibility. The results of this work support this hypothesis and showed that crosslinking electrospun chitosan with genipin slowed degradation of mats by 17 % and improved initial mechanical properties by 165% percent as compared to uncrosslinked mats, and that crosslinked mats were compatible with cells and did not impact cellular growth. The addition of genipin also had a slight effect on the mean nanofiber diameter of the electrospun mats.

In this study, we electrospun 5.50% chitosan in 70% TFA and 30% DCM. Our study found the average nanofiber diameter to be 162-228 nm for uncrosslinked chitosan and slightly lesser diameters (142-197 nm) for crosslinked membranes. These results are in agreement with others who electrospun chitosan using similar methods and found mean fiber diameters between 77 to 330 nm [12, 19, 20]. The TFA solvent forms salts with the amino group of the chitosan molecules which destroys the rigid interactions between chains thus allowing electrospinning [14]. As the polymer is crosslinked with genipin, there is a decrease in free amino groups, which displaces the TFA salt and alters polymer chain interactions thus resulting in thinner fibers being formed as compared to the uncrosslinked material.

To crosslink chitosan nano-fibers, other researchers have added small amounts of glutaraldehyde liquid to the chitosan polymer solution [13]. They found that adding

glutaraldehyde to the chitosan solution increased the mean fiber diameter from  $77 \pm 29$  nm for as spun fibers to  $128 \pm 40$  nm. Furthermore, when glutaraldehyde vapor was used to crosslink chitosan fibers after electrospinning, the diameter increased even more to  $172 \pm 75$  nm [12]. The crosslinking with glutaraldehyde also resulted in significantly decreased mechanical strength of the chitosan mats [12]. Our study demonstrated that when genipin was used to crosslink the fibers, there was no increase in fiber diameter, and more importantly, there was an increase in mechanical strength. The results from our study indicate that genipin helps to maintain small fiber diameters and to retain the desired topographical scale and cell occlusive properties of the mat, as well as maintain adequate mechanical properties for clinical handling and manipulating the mats.

The degradation study demonstrated that genipin crosslinking may be used to extend the degradation of electrospun chitosan membranes. The 5 mM and 10 mM crosslinked membrane groups showed a slower degradation rates with 8-17% less mass loss, respectively, at 16 weeks as compared to uncrosslinked mats. These data provide evidence genipin crosslinking reduces rate of degradation of membranes and that all groups meet the 4-6 month target timeframe. However, it is also important to note that our uncrosslinked membranes usually fragmented sometime after 4 weeks in solution while our crosslinked membranes did not. This indicates that even though uncrosslinked mats may have degradation rates on par with the 4-6 month time frame, crosslinked mats may perform better in GBR applications since fragmented uncrosslinked membranes would be unable to provide an effective barrier function. These *in vitro* data are predictive of the chitosan mats meeting degradation target timeframes, and that the genipin crosslinked membranes will remain intact. Differences in degradation rates

would be expected *in vivo*, and this *in vitro* evaluation should only be used to rank the degradation profiles.

Sangsanoh et al. evaluated the *in vitro* weight loss of electrospun chitosan membranes over 12 weeks and had comparable results using PBS without lysozyme [11]. However, they observed a slightly slower degradation rate with 14 % mass loss at 4 weeks and 16.5% mass loss at 12 weeks for uncrosslinked mats, while we observed 21 % mass loss at 4 weeks and 34% mass loss at 16 weeks for uncrosslinked mats. These differences are most likely due to the presence of lysozyme in our PBS solution, the primary enzyme responsible for chitosan degradation [21]. *In vivo* studies by Shin et al. reported membrane fragmentation and rapid degradation after 8 weeks when uncrosslinked electrospun chitosan mats made using HFIP were implanted in rat subcutaneous tissue [9]. Our electrospun membranes, and those evaluated by Sangsanoh et al., were constructed using TFA/DCM solvent system and used higher weight percent chitosan (5.5% and 7% vs. 1.5% (w/v) chitosan) and were neutralized, so our results may not be directly comparable. It is important to note that neutralization may play a large role in the degradation of these mats by causing protonation of the chitosan polymer. Protonation grants a positive charge to the polymer and renders it insoluble in aqueous solutions, which probably contributes to the slower degradation.

The strength of the mats in this study without crosslinking was 3 times greater than those reported by Schiffmann et al. who studied un-neutralized electrospun chitosan mats with and without crosslinking using glutaraldehyde. Additionally, Schiffmann et al. used a 2.7 % (w/v) chitosan solution, 83% DDA, ~190-310 kDa, a spinning distance of 6.4 cm, and pure TFA solvent, while this study evaluated 5.5% (w/v) chitosan solution,

70 % DDA, 312 kDa, a spinning distance of 15 cm, and 70/30 TFA/DCM solvent mixture. The previous studies by Schiffmann et al. showed that using glutaraldehyde to crosslink decreased the ultimate tensile strength from 4 MPa to around 1 MPa and increased the brittleness of the membrane [12]. Our results demonstrated significantly higher ultimate tensile stress when genipin was used to crosslink from 12 MPa for uncrosslinked to 32 MPa for 10 mM crosslinked (Figure 3). The fiber diameters, when comparing uncrosslinked chitosan mats, differed between the two methods (77 vs 198 nm). The observed differences in mechanical strength of uncrosslinked membranes between the current study and the one performed by Schiffmann et al. could be attributed to the differences in electrospinning parameters, fiber size, or to the neutralization process. The increase in tensile strength observed in this study was attributed to the genipin crosslinking of the chitosan material (as evidenced by FTIR), was significant for the 10 mM concentration and almost significant for the 5 mM concentration ( $p=0.06$ ). These results indicate that genipin crosslinking of chitosan mats is an effective method to increase the ultimate strength for improved clinical handle-ability.

Under the acidic crosslinking conditions of this study, genipin will bind the amino group on the chitosan chain, to which another genipin molecule will attach, to form dimer, trimer and tetramer bridges of genipin between and within chitosan chains [16, 17]. Therefore, we would expect to see a decrease in the amount of free amino groups present when genipin crosslinking occurs. FTIR did show that peaks associated with N-H stretch at  $3372\text{ cm}^{-1}$  were diminished in intensity as the level of crosslinking increased, indicating that genipin was binding chitosan at the amino group. From the normalized absorbance spectra we can see the height of the N-H peak decreased by 60% for 5 mM

genipin crosslinked and decreased by 86% for 10 mM crosslinked. This decrease indicates that genipin is interacting with the chitosan at the amino group in a dose dependent manner. Thus, crosslinking is the mechanism by which we observed the proportional increase in mechanical strength and degradation time with genipin concentration in the electrospinning solution.

The five-day cell growth study demonstrated that the chitosan membrane is cytocompatible and will not inhibit osteoblast proliferation. The proliferation and viability was unaffected by crosslinking degree and the cell morphology was mostly cuboidal but there was some cell spreading along the fibers in the less densely populated areas on the membrane (Figure 6B). The overwhelming majority of cells were healthy and viable. These results are in agreement with Sangsanoh et al. who evaluated Schwann cell proliferation on uncrosslinked chitosan films and electrospun fibers over a five-day period. Their study demonstrated similar capacity for the chitosan films and fibers to support cell proliferation over the 5 day period and mostly cuboidal cell morphology [19]. Our results illustrate for the first time that genipin can be used to crosslink electrospun chitosan fibers to increase the mechanical properties, maintain nano-fibrous morphology, and support cellular proliferation.

## **5. Conclusion**

These results suggest that electrospun chitosan mats may benefit from crosslinking with genipin. This study has demonstrated that electrospun chitosan mats, with and without genipin crosslinking, have mechanical properties, degradation rate, and cytocompatibility which are sufficient for GBR applications. Crosslinking with genipin may offer increased mechanical strength and increased cycompatibility compared to other crosslinkers. These findings warrant expanded *in vitro* and *in vivo* investigations into genipin-crosslinked electrospun chitosan mats for GBR applications.

## References

1. Chiapasco M, Zaniboni M (2009) Clinical outcomes of GBR procedures to correct peri-implant dehiscences and fenestrations: a systematic review. *Clin Oral Implants Res* 20(Sppl 4):113-23
2. Strietzel FP (2001) [Risks and complications of membrane-guided bone regeneration. Retrospective analysis]. *Mund Kiefer Gesichtschir* 5(1):28-32
3. Clarizio LF (1999) Successful implant restoration without the use of membrane barriers. *J Oral Maxillofac Surg* 57(9):1117-21
4. Moses O, Vitrial D, Aboodi G, Sculean A, Tal H, Kozlovsky A, Artzi Z, Weinreb M, Nemcovsky CE (2008) Biodegradation of three different collagen membranes in the rat calvarium: a comparative study. *J Periodontol* 79(5):905-11
5. Tal H, Kozlovsky A, Artzi Z, Nemcovsky CE, Moses O (2008) Long-term biodegradation of cross-linked and non-cross-linked collagen barriers in human guided bone regeneration. *Clin Oral Implants Res* 19(3):295-302
6. Becker W, Dahlin C, Becker BE, Lekholm U, van Steenberghe D, Higuchi K, Kultje C (1994) The use of e-PTFE barrier membranes for bone promotion around titanium implants placed into extraction sockets: a prospective multicenter study. *Int J Oral Maxillofac Implants* 9(1):31-40
7. Bornstein MM, Bosshardt D, Buser D (2007) Effect of two different bioabsorbable collagen membranes on guided bone regeneration: a comparative histomorphometric study in the dog mandible. *J Periodontol* 78(10):1943-53
8. Kuo SM, Chang SJ, Chen TW, Kuan TC (2006) Guided tissue regeneration for using a chitosan membrane: an experimental study in rats. *J Biomed Mater Res A* 76(2):408-15
9. Shin SY, Park HN, Kim KH, Lee MH, Choi YS, Park YJ, Lee YM, Ku Y, Rhyu IC, Han SB, Lee SJ, Chung CP (2005) Biological evaluation of chitosan nanofiber membrane for guided bone regeneration. *J Periodontol* 76(10):1778-84
10. Yeo YJ, Jeon DW, Kim CS, Choi SH, Cho KS, Lee YK, Kim CK (2005) Effects of chitosan nonwoven membrane on periodontal healing of surgically created one-

wall intrabony defects in beagle dogs. *J Biomed Mater Res B Appl Biomater* 72(1):86-93

11. Sangsanoh P, Supaphol P (2006) Stability improvement of electrospun chitosan nanofibrous membranes in neutral or weak basic aqueous solutions. *Biomacromolecules* 7(10):2710-4
12. Schiffman JD, Schauer CL (2007a) Cross-linking chitosan nanofibers. *Biomacromolecules* 8(2):594-601
13. Schiffman JD, Schauer CL (2007b) One-step electrospinning of cross-linked chitosan fibers. *Biomacromolecules* 8(9):2665-7
14. McIlwee HA, Schiffman JD, Cathell MD, Schauer CL, Deposition of chitosan: thin films and fibers, in *Current Research and Developments on Chitin and Chitosan in Biomaterials Science*, R. Jayakumar and M. Prabaharan, Editors. 2008, Research Signpost: Kerala, India. p. 82-122.
15. Pham QP, Sharma U, Mikos AG (2006) Electrospinning of polymeric nanofibers for tissue engineering applications: a review. *Tissue Eng* 12(5):1197-211
16. Mi FL, Tan YC, Liang HC, Huang RN, Sung HW (2001) In vitro evaluation of a chitosan membrane cross-linked with genipin. *J Biomater Sci Polym Ed* 12(8):835-50
17. Mi FL, Tan YC, Liang HF, Sung HW (2002) In vivo biocompatibility and degradability of a novel injectable-chitosan-based implant. *Biomaterials* 23(1):181-91
18. Chang WH, Chang Y, Lai PH, Sung HW (2003) A genipin-crosslinked gelatin membrane as wound-dressing material: in vitro and in vivo studies. *J Biomater Sci Polym Ed* 14(5):481-95
19. Sangsanoh P, Waleetorncheepsawat S, Suwantong O, Wutticharoenmongkol P, Weeranantanapan O, Chuenjitbuntaworn B, Cheepsunthorn P, Pavasant P, Supaphol P (2007) In vitro biocompatibility of schwann cells on surfaces of biocompatible polymeric electrospun fibrous and solution-cast film scaffolds. *Biomacromolecules* 8(5):1587-94

20. Ohkawa K, Cha D, Kim H, Nishida A, Yamamoto H (2004) Electrospinning of Chitosan. *Macromol Rapid Commun* 25:1600-1605
21. Varum KM, Myhr MM, Hjerde RJ, Smidsrod O (1997) In vitro degradation rates of partially N-acetylated chitosans in human serum. *Carbohydr Res* 299(1-2):99-101

**CHAPTER 3: Submission to the Journal of Biomedical Materials Research:  
Part A**

**Suture pullout strength and *in vitro* fibroblast and RAW 264.7 monocyte biocompatibility of genipin crosslinked nano-fibrous chitosan mats for guided tissue regeneration.**

Authors: Norowski, PA, Mishra, S, Adatrow, PC, Haggard, WO, Bumgardner, JD.

**Abstract:** Chitosan materials have been advocated for guided tissue regeneration (GTR) applications because of their biocompatibility, degradability, wound healing and osteogenic properties. In this study, electrospun chitosan membranes, crosslinked with 5 mM or 10 mM genipin, a natural crosslinker derived from the gardenia plant, were evaluated for suture pullout strength, crystallinity and cytocompatibility with normal human dermal fibroblast and TIB 71<sup>TM</sup> RAW 264.7 monocyte cells. Ultimate suture pullout strength was significantly lower (51-67%) than that of commercially available collagen membranes (BioMend Extend, Zimmer Dental). Crystallinity of the electrospun chitosan mats decreased upon crosslinking by 14-17% (p=0.013). Uncrosslinked and crosslinked chitosan mats were biocompatible and supported fibroblast cell proliferation over 9 days without allowing cell penetration. Finally, chitosan membranes inhibited lipopolysaccharide (LPS)-induced RAW 264.7 nitric oxide production by 59-67% as compared to tissue culture plastic and collagen membrane. Membranes demonstrated cytocompatibility with fibroblasts and did not activate monocytes to produce pro-inflammatory factors *in vitro*. In monocyte cultures with LPS, activation of monocytes grown on electrospun chitosan membranes was reduced as indicated by NO production normalized to cell number as compared to tissue culture plastic and commercially-available glutaraldehyde-crosslinked collagen membrane controls. Improvements are needed in the tear strength of electrospun chitosan membranes for clinical application.

However, the ability of chitosan to inhibit LPS-induced NO expression in monocytes may be beneficial in the treatment of patients with chronic periodontitis who are undergoing GTR procedures.

## **INTRODUCTION**

Guided tissue regeneration (GTR) is a surgical technique used to direct the formation of bone by using a barrier membrane to exclude the faster healing soft tissues from the graft site. While the use of barrier membranes is expanding into other surgical arenas, in dentistry, they are primarily used to treat intrabony defects caused by periodontal lesions around teeth or implants. In oral/maxillofacial surgery they are used to protect the graft space in larger bone defects caused by bone resection, bone atrophy, trauma, or osteotomy. Currently utilized materials for GTR are non-ideal because they either require an additional removal surgery or they do not resorb predictably in a manner that matches the surrounding tissue remodeling rates. Ideally, GTR membranes provide effective barrier function to maintain tissue spaces, allow for diffusion of nutrients, wastes and signaling factors during healing and degrade on a time scale consistent with healing and tissue maturation.

Chitosan is a linear biopolymer composed of more than 50% N-glucosamine units in a N-acetyl-glucosamine –co- N-glucosamine copolymer. Chitosan materials have been advocated for GTR applications because of their biocompatibility, controllable biodegradation, and non-toxic degradation products<sup>1-3</sup> and have been manufactured into fibers and sheets using a variety of techniques including electrospinning, wet-spinning, and solution casting.<sup>1-6</sup> Electrospinning, which uses a high voltage source to fabricate polymer fibers, is well suited for the production of fibrous membranes because it is

relatively inexpensive, simple, and can reliably reproduce fibers in the nano-range.

Nano-fibrous membranes are particularly advantageous in GTR because they allow fluid and nutrient exchange through the membrane while maintaining a porosity that is small enough to be cell occlusive.<sup>7-10</sup> Electrospun materials are also thought to mimic the topology of the extracellular matrix, promoting cell attachment and proliferation.<sup>11-13</sup>

Using electrospinning techniques, Shin et al. made nanofibrous GTR membranes to be biomimetic and provide cell occlusion.<sup>2</sup> They demonstrated that the electrospun chitosan membranes facilitated more new bone formation in critical size bone defects than control (empty defect) after 4 weeks in rabbit calvaria.<sup>2</sup> However, they noted that their electrospun chitosan membranes fragmented after 8 weeks of implantation in rat subcutaneous tissue. These studies demonstrated the potential of degradable chitosan membranes to maintain graft space and regenerate bone with minimal inflammatory response<sup>1-3</sup> but improvements must be made in the clinical handle-ability and strength of electrospun chitosan membranes in order to improve clinical outcomes.

Glutaraldehyde crosslinking has been advocated for increased stability and strength of electrospun chitosan membranes but caused an increase in the average fiber diameter, did not increase the ultimate tensile strength of the chitosan membranes, nor did the investigators evaluate degradation or biocompatibility.<sup>5,6</sup> Recently, we have shown that crosslinking electrospun chitosan membranes with 5 or 10 mM genipin decreased *in vitro* degradation kinetics to have 78%-66% percent mass remaining at 16 weeks which would predict a degradation timeframe that is on target with recommendations by clinicians. Additionally, the genipin crosslinking increased tensile

strengths of the electrospun mats by 260% which were also cytocompatible with SAOS-2 osteoblastic cells [Norowski et al., in review].

Periodontitis is a chronic inflammatory disease in which the host response is primarily driven by the presence of lipopolysaccharide (LPS) which causes monocyte recruitment and differentiation into macrophages and pre-osteoclasts, ultimately leading to bone and soft tissue breakdown.<sup>14</sup> Patients with periodontitis also have elevated expression of nitric oxide (NO) in the gingival and periodontal ligament tissues.<sup>15-17</sup> While currently available GTR membrane materials do not actively participate in the treatment of periodontitis, bioactive materials may provide advantages if they are able to lessen or inhibit tissue destruction associated with LPS-induced chronic inflammation or inhibit NO production.<sup>15-17</sup> Chitosan oligosaccharide and other chitinous constructs have been shown to inhibit NO production by RAW 264.7 monocytes and other inflammatory cells.<sup>18-21</sup>

In this study, the natural crosslinker genipin, which is isolated from the fruit of the gardenia plant, was used to crosslink chitosan nanofibrous mats. Past studies have shown that chitosan and gelatin membranes were more biocompatible, less inflammatory, and resulted in faster healing times when crosslinked with genipin instead of glutaraldehyde.<sup>22-24</sup> Our goal was to characterize genipin-crosslinked electrospun-chitosan membranes and evaluate their potential performance as GTR membranes as compared to commercially available degradable collagen membranes. Electrospun chitosan membranes should not exhibit cytotoxicity to human fibroblast cells nor activate monocyte inflammation.

## **MATERIALS AND METHODS**

### **Electrospinning procedure**

Nanofibrous chitosan mats with random fiber orientation were fabricated by electrospinning. Briefly, a 5.50(wt/v)% chitosan solution in 70(v/v)% trifluoroacetic acid and 30(v/v)% methylene chloride was gently mixed overnight. Genipin was mixed into the polymer solution 30 minutes prior to the start of electrospinning at a concentration of 0, 5, or 10 mM. The solution was loaded into a 10 mL syringe with a blunt 20G, 3.81 cm stainless steel needle tip. The syringe was loaded into a syringe pump and the flowrate set to 20  $\mu\text{L}/\text{min}$ . The solution was electrospun at 25 kV and the fibers were collected on a non-stick aluminum foil target (38.1 cm diameter circular disc), positioned 15 cm from needle tip and rotated at 8.4 RPM by an AC motor to ensure even and random distribution of fibers. The electrospinning apparatus was housed inside a ventilated box, which was vented to the fume hood. After electrospinning, the nano-fibrous mat was put under vacuum overnight to remove residual solvent, carefully removed from the foil, and then neutralized in room temperature 5M  $\text{Na}_2\text{CO}_3$  (saturated solution) for 3 hours.<sup>4</sup> The membrane was then rinsed with deionized water until neutral. After drying at ambient conditions, mats were sterilized using ethylene oxide gas.

### **Suture pullout strength**

Suture pullout tests were performed to determine the tear strength of the membranes. Membrane specimens were prepared to be 10 mm wide and about 40 mm long. As a comparison to currently-available clinically-used materials, electrospun mats were tested against a degradable collagen membrane crosslinked with glutaraldehyde (Biomend Extend, Zimmer Dental, Warsaw IN, USA). A single suture was made 5 mm from the

top edge and 5 mm from each side. The suture was a 70 cm general closure monofilament polydioxanone (PDS II, Ethicon, Z-341) with taper ct-1 needle and 1 (4.0 metric) gauge. The suture was left un-knotted but was affixed to the upper claw of the Instron™ model 4465 mechanical test frame (Norwood, MA, USA) (Figure 1). Suture pullout testing (n=4) of dry specimens was carried out with a 50 N load cell and an extension rate of 1 mm/min. Maximum load was recorded in Newtons (N) and normalized to membrane thickness.

### **X-ray diffraction (XRD)**

Crystallinity measurements were made using Bruker D8 Advance XRD. Chitosan membranes were ground into a fine powder with a mortar and pestle, after submersion in liquid nitrogen. Powders were scanned in grazing angle reflection mode and data were collected with  $2\theta$  from 4 to 30. Crystallinity index was determined by taking the difference of the peak intensity that occurs at  $2\theta=20$  and the lowest point of the baseline (amorphous region) of the spectrum ( $2\theta=10$ ) then normalizing to the peak intensity.<sup>25</sup>

### **Molecular weight measurement by size exclusion chromatography coupled with multi-angle static light scattering (SEC-MALS)**

Chitosan samples were run at 30 °C, through 2 TSK gel columns in series (polymer range 100,000-900,000) with a mobile phase of 0.15 M HAc and 0.1 M NaAc (pH 5). Chitosan was dissolved at 1 mg/mL, filtered using a 0.45  $\mu\text{m}$  pore size, and injected using 50  $\mu\text{L}$  injection volume. The molecular weights,  $M_w$  and  $M_n$ , were determined using multi-angle static light scattering (Wyatt, Dawn HELEOS II) and a refractive index detector (Varian, Prostar 450). The  $dn/dC$  for chitosan was entered as  $0.163 \text{ mL}^{-1}$  as previously reported.<sup>26</sup> All analysis performed using ASTRA software (Wyatt Technologies Corp.).

Measurements were made on the starting material and the uncrosslinked membrane, but no measurements could be made of crosslinked membranes as they did not go into solution in the mobile phase, even with increased acidity.

### **Fibroblast cytocompatibility**

Normal human dermal fibroblasts (NhDF) (ATCC No. PCS-201-010, Manassas, VA, USA) cells were seeded on uncrosslinked and crosslinked nanofibrous membranes mounted in 24-well size CellCrown™ culture inserts (Scaffdex, Tampere, Finland). CellCrown™ inserts were used to keep membranes from floating in culture wells and to provide a uniform and flat surface for cell culture. Membranes were rinsed in culture media 4 times and then seeded at  $1 \times 10^5$  cells per membrane. Cells were also seeded onto 24-well tissue culture plastic as a positive control. Cells were grown in Dubulco's modified eagle medium (DMEM) supplemented with 10% fetal bovine serum (FBS) and 500 I.U./mL penicillin, 500  $\mu\text{g}/\text{mL}$  streptomycin, and 2.5  $\mu\text{g}/\text{mL}$  amphotericin-B. Proliferation was measured at days 1, 5, and 9 (n=4 per group per time point) using Cell Titre Glo™ luminescent cell viability assay (Promega, Madison, WI, USA). The assay measures the number of cells based on the amount of light produced from the oxidation of intracellular ATP in the luciferin-luciferase reaction. Cell number was determined by means of a standard curve of NhDF cells in 24 well plates.

### **Monocyte activation**

TIB 71™ RAW 264.7 monocyte cells were seeded on uncrosslinked, genipin-crosslinked, and commercially available collagen membranes (Biomend Extend, Zimmer Dental, Warsaw In) or tissue culture plastic as control. Scaffolds (n=4) were seeded at  $1.0 \times 10^6$  cells per scaffold. Cells were grown in DMEM supplemented with 10% FBS,

and 500 I.U./mL penicillin, 500 µg/mL streptomycin, and 25 µg/mL amphotericin-B. All treatment groups were grown in the presence or absence of 1 µg/mL lipopolysaccharide (LPS, *Escherichia coli* derived). LPS is known to stimulate monocyte cells to produce the reactive oxygen species, nitric oxide (NO), a potent signaling and pro-inflammatory molecule. The cumulative levels of NO produced by the cells on the membranes was measured via the Griess Reagent (Promega, Madison, WI, USA) as an indicator of monocyte stimulation on days 1, 2 and 3. The viability of cells was measured at the terminal timepoint (day 3) to verify cell number using Cell Titre Glo™ luminescent cell viability assay. Cell number was determined by means of a standard curve of RAW 264.7 cells in 24 well plate.

Statistically significant differences were detected by one-way or two-way ANOVA followed by Student-Neuman-Kools (SNK) post-hoc test to determine where differences existed between groups. Statistical significance was declared at  $p < 0.05$ .

## **RESULTS**

Suture pullout tests were carried out using monofilament polydioxanone suture (Figure 1). Specimens showed predictable tear patterns that extended upwards toward the superior edge of the specimen (Figure 2). Ultimate load per mm thickness measurements demonstrated that electrospun chitosan membranes did experience a 48% increase in tear strength with 10 mM genipin crosslinking which was not significant (Figure 3). However, the strength exhibited by the chitosan membranes was less than the commercially available glutaraldehyde-crosslinked collagen membranes. Even at the higher 10 mM concentration of genipin, the ultimate load was 51% of the BioMend Extend. Crystallinity measurements made by XRD showed that chitosan decreased in

crystallinity with crosslinking by 15-17% ( $p=0.013$ ) with no significant difference between the 2 levels of crosslinking (Table 1). Molecular weight measurements revealed that chitosan chain length is decrease upon electrospinning from 311 kDa to 77 kDa (Table 2).

The fibroblast growth study indicated that cells were able to attach and proliferate on the chitosan membranes (Figure 4). There were no differences detected between the different levels of genipin crosslinking with respect to fibroblast growth.

Results from the TIB 71<sup>TM</sup> RAW 264.7 monocyte culture indicate that the chitosan and collagen membranes are not pro-inflammatory. All NO levels from cells seeded on membrane materials were lower than those on tissue culture plastic (Figure 5). Additionally, in the presence of LPS, NO secretion by the monocyte cells was reduced by the chitosan and collagen membranes (Figure 6). On day 1, the type I collagen membranes reduced NO release by 97% and the chitosan membranes (un-cross-linked or cross-linked) reduced NO release by 59-68%. On day 2, the type I collagen membranes reduced NO release by 107% and the chitosan membranes (un-cross-linked or cross-linked) reduced NO release by 53-60%. On day 3, the type I collagen membranes reduced NO release by 106% and the chitosan membranes reduced NO release by 50-60%. At the day 3 terminal timepoint, viability measurements made in a separate experiment using Cell Titre GLO<sup>TM</sup> revealed that the viability of cells on glutaraldehyde-crosslinked collagen was lower than control and cells growing on chitosan membranes (Figure 7).

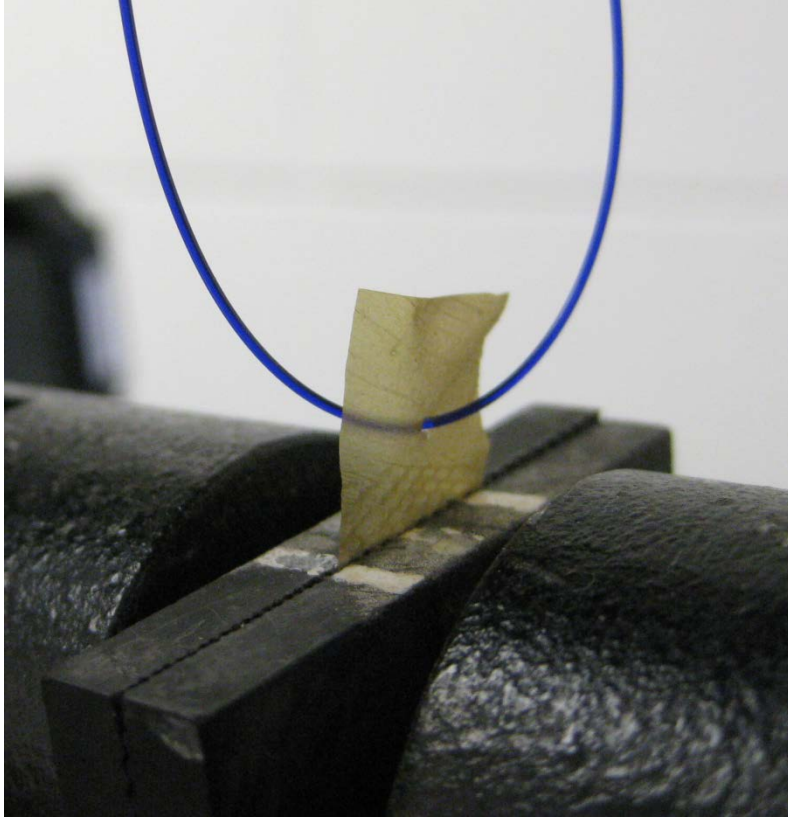


**Figure 1 – Suture pullout tests were conducted at 1 mm/min extension rate and maximum load was recorded (n=4).**

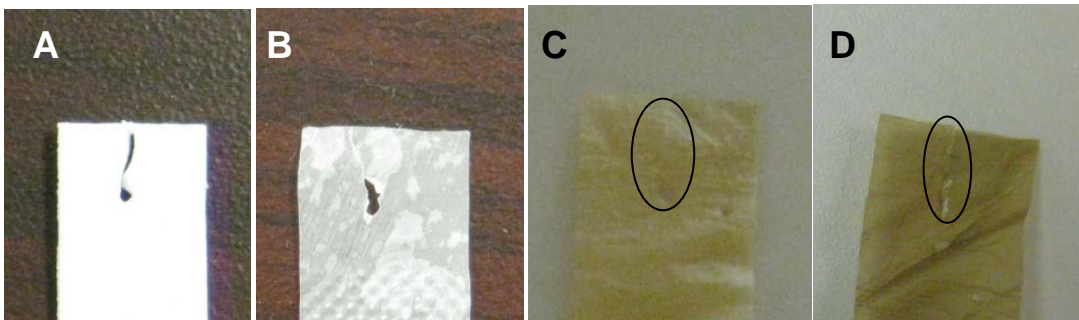


**Figure 2 – Torn specimens after suture pullout for A) Collagen membrane B) Electrospun chitosan membrane C) 5 mM genipin-crosslinked electrospun chitosan and D) 10 mM genipin-crosslinked electrospun chitosan. Circles are drawn to highlight the material tear. All specimens tore as expected towards the upper edge.**

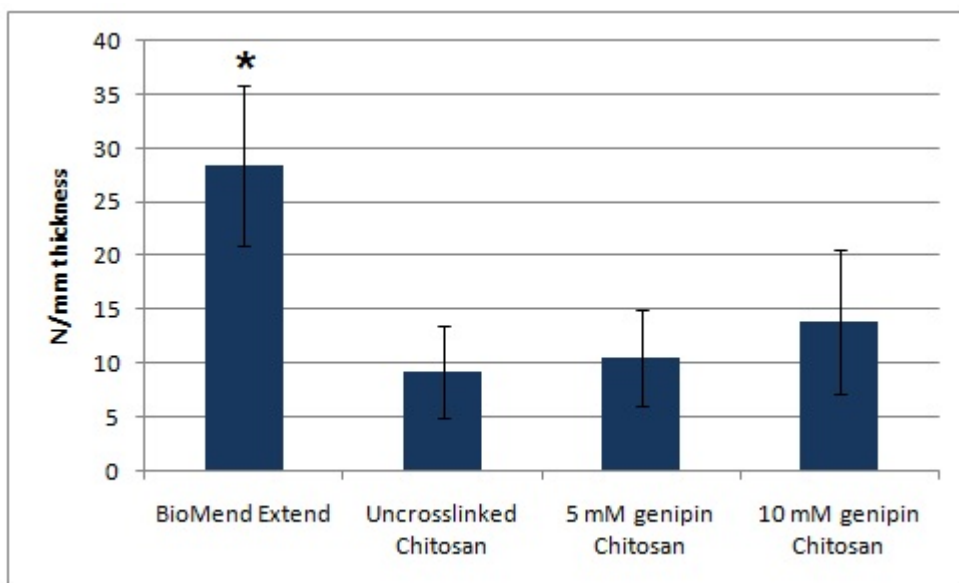


**Figure 3 – Ultimate suture pullout load normalized to membrane thickness of the electrospun membranes showed no significant increase in strength with crosslinking. All test membranes tore at lower loads than commercially available collagen membrane (n=4).**

**TABLE 1 – Crystallinity of the nanofibrous membranes ground into coarse powder and analyzed by XRD. Note that uncrosslinked membranes exhibited the largest crystalline peak at  $2\theta=20$  (\* indicates significance,  $p=0.013$ ).**

<i>Groups</i>	<i>Average CI (%)</i>	<i>Standard Deviation</i>
Uncrosslinked	37.0 (*)	6.1
5 mM genipin	20.9	3.0
10 mM genipin	23.1	8.9

**TABLE 2 – Molecular weight (Mw) Molecular number (Mn) and polydispersity index (PDI) of chitosan before and after electrospinning using TFA/DCM.**

	Mw	Mn	PDI
Starting material	311,500	239,200	1.30
Electrospun material	77,270	54,400	1.42

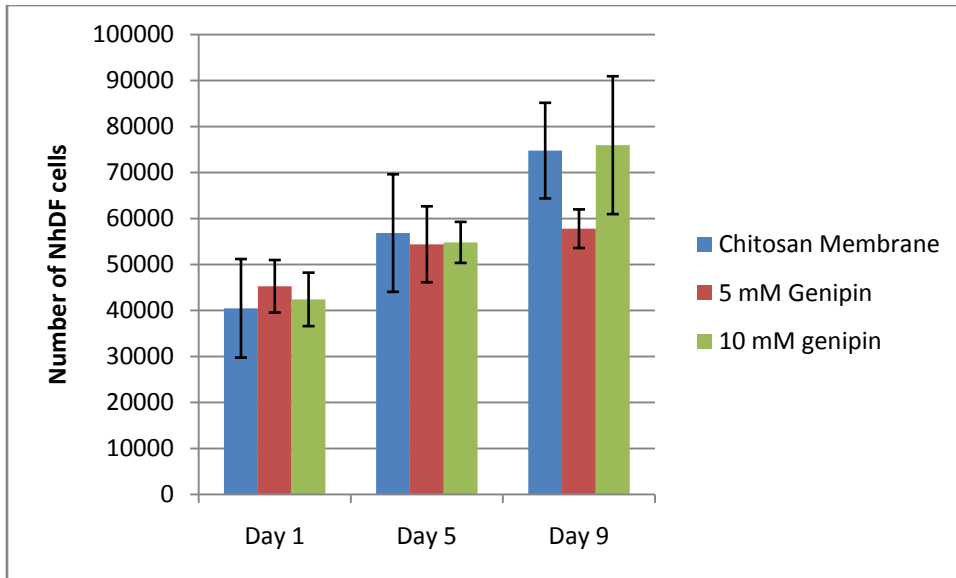


**Figure 4 – NhDF proliferation over nine days demonstrated cytocompatibility and there was no significant difference between the groups (n=4).**

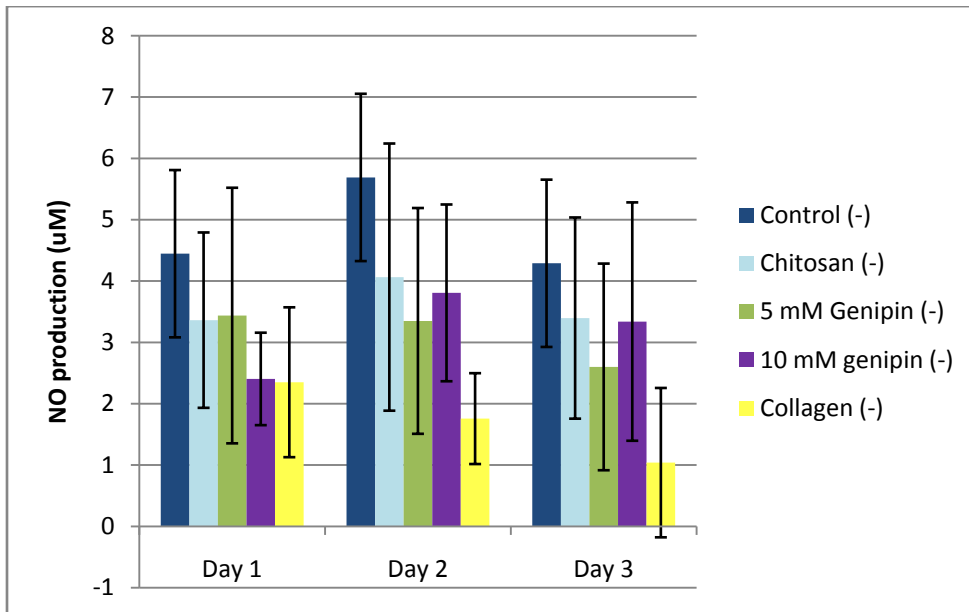


**Figure 5 – NO production in the absence of LPS by RAW 264.7 cells seeded on tissue culture plastic (control) test and commercially available GBR membranes (collagen). In the absence of LPS, test materials did not stimulate NO production compared to control.**

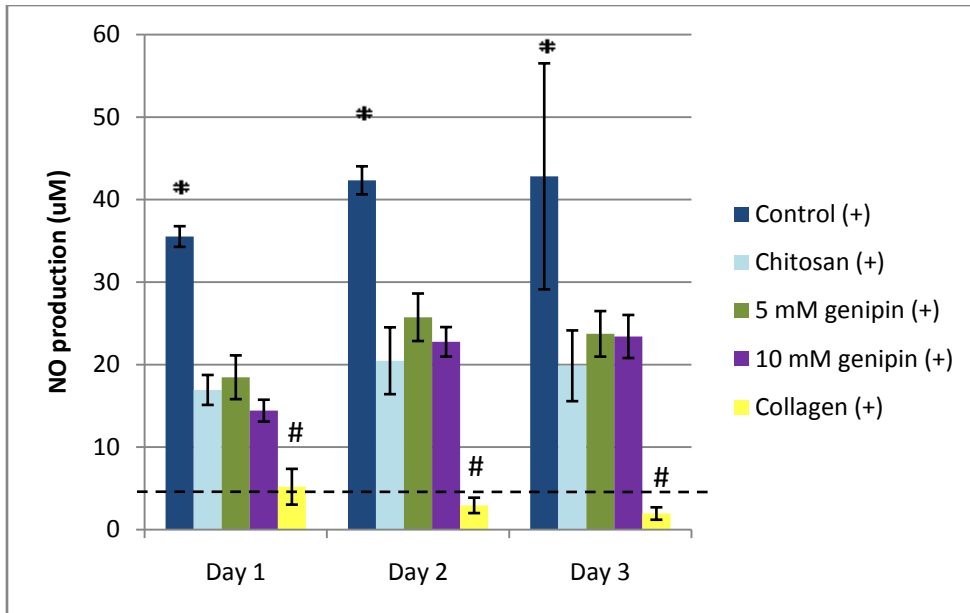


**Figure 6 – NO production in LPS stimulated RAW 264.7 monocyte cells on tissue culture plastic (control), test materials and commercially available GTR membrane. Tissue culture plastic (control) produced significantly more NO than cells on chitosan or collagen GTR membranes when stimulated with LPS (n=4). However, the NO levels on measured from the glutaraldehyde-crosslinked collagen group may have been low due to low cell viability. Dotted line shows baseline expression as measured from unstimulated control cells (figure 5).**

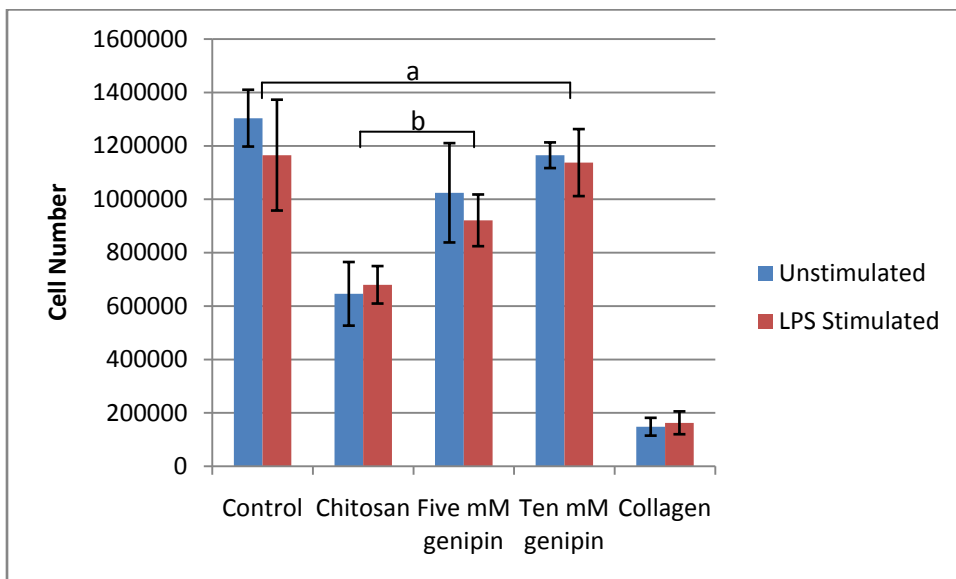


**Figure 7 – Viability of RAW 264.7 monocyte cells measured at the day 3 terminal timepoint. There was no effect with LPS treatment. Viability on glutaraldehyde-crosslinked collagen membrane was significantly lower than other groups (a and b) ( $p=3.8 \times 10^{-13}$ ). Viability also appears low on uncrosslinked chitosan but this may have been due to interference caused by membrane dissolution during the assay.**

## DISCUSSION

Tensile testing in a previous study showed dose dependent improvement in tensile strength with genipin-crosslinking [Norowski et al., in review]. However, in the suture pullout test only a modest and insignificant increase from 9.3 to 13.8 N/mm in tear ultimate load was observed with genipin crosslinking. One explanation as to why genipin crosslinking benefited the tensile strength but did not benefit the tear strength is that these are thin polymer membranes which are not resistant to tearing once a defect is introduced. When the suture is placed, a tear is introduced in the membrane and the small, non-woven, fibers do not offer substantial resistance to tear propagation. Further, the tear strengths of the chitosan membranes were significantly less than that of the BioMend Extend crosslinked collagen membranes tested. It should be noted that the thickness of the BioMend Extend is significantly greater than the chitosan membrane (0.39 vs 0.05 mm). BioMend Extend is designed to be thicker than other collagen membranes for a longer duration of degradation: 18 weeks as opposed to 8 weeks for BioMend (Zimmer product description). However, even when maximum load is normalized to membrane thickness, the strength of electrospun chitosan membranes was well below that of type 1 collagen. Increased suture pullout strength could possibly be achieved by increasing fiber entanglement/adhesion of the membrane.

Results from the XRD suggest that genipin crosslinking reduces crystallinity by disrupting chain packing of the chitosan. This is commonly seen for crosslinked polymer materials. Results from the SEC-MALS indicate that the chitosan polymer is decreasing in molecular weight during the electrospinning process. This reduction can be explained by the solvents used to electrospin, which may cause chain scission. Unfortunately, the

crosslinked membranes did not go into solution using various concentrations of acetic acid, nor HCl, so measurements were not possible. Reduced crystallinity and molecular weight may have contributed to lower fiber mechanical properties which contributed to the low tear strengths measured in this study.

The nine-day fibroblast growth study demonstrated that the chitosan membrane is cytocompatible and will not inhibit fibroblast proliferation. The attachment and growth of NhDF cells were unaffected by crosslinking degree. Sangsanoh et al., who evaluated Schwann cell proliferation over a five-day period on uncrosslinked chitosan electrospun mats, demonstrated a similar capacity for the chitosan nanofibrous mats to support cell proliferation.<sup>27</sup> These results are in agreement with our previous studies which showed that genipin-crosslinked electrospun chitosan mats were not cytotoxic to SAOS-2 osteoblastic cells [Norowski et al., in review]. It was also reported that genipin crosslinking of electrospun silk fibroin/hydroxybutyl chitosan resulted in cytocompatible materials when tested for wound healing in rats and *in vitro* cytocompatibility.<sup>28</sup> These studies demonstrated the *in vitro* biocompatibility of the electrospun chitosan mats and genipin-crosslinked electrospun chitosan mats.

The chitosan membranes in the RAW 264.7 monocyte study did not stimulate cells to produce NO in the absence of LPS. Viability measurements revealed that viability was not dependent on LPS stimulation, but that the glutaraldehyde crosslinked collagen membrane did have lower viability than cells on chitosan membranes or tissue culture plastic ( $p=3.8 \times 10^{-13}$ ). The Biomend Extend collagen membrane also exhibited low levels of NO production in the absence of LPS which may have been caused by low cell viability. Bovine type I collagen has also been reported to interact with RAW 264.7

monocyte cells by inhibiting or halting their proliferation and cell division.<sup>29</sup> This was noted in our study because of low viability in both unstimulated and LPS-stimulated cells grown on BioMend Extend membranes. In addition, the media in the collagen membrane groups did not change color to yellow due to metabolic activity like all other wells, but instead stayed the initial red color. Bovine, but not rat or murine, type I collagen has also been reported to stimulate NO production in RAW 264.7 cells<sup>30</sup> and to modulate the effects of other factors such as osteopontin in the presence of LPS stimulation.<sup>31</sup> This interaction of the murine cells on bovine collagen may have been responsible for the decreased viability observed; however, glutaraldehyde crosslinking may have also contributed to the low viability.

In LPS-stimulated groups, electrospun chitosan membranes reduced NO production by RAW 264.7 cells. This effect has been reported in other studies using chitosan oligosaccharide with RAW 264.7 and other inflammatory cell types.<sup>18-21,32</sup> These studies have noted that the ability of chitosan to reduce NO production is dependent on chitosan chain length, water-solubility, and also the nano-structure since chitosan nanoparticles, and high molecular weight water-soluble chitosans were reported to stimulate RAW 264.7 cells to produce NO at levels similar to positive control of LPS or TNF- $\alpha$ .<sup>33-35</sup> The ability of chitosan to inhibit monocyte activation has been attributed to competitive binding of the surface receptor of the LPS ligand. Once chitosan has bound the receptor, the MW, solubility, and nano-architecture play a role in whether the receptor is activated or inactivated.<sup>18,19</sup> In general, lower molecular weight chitosans are reported inhibit NO production, while higher molecular weight and water soluble chitosans stimulate monocytes to produce NO.<sup>35</sup> In this study, electrospun chitosan mats

have both a low Mw, around 73 kDa after electrospinning, and low solubility due to neutralization and crosslinking processes, which may have contributed to its ability to inhibit NO production. Genipin-crosslinked electrospun-chitosan membranes suppressed LPS-induced monocyte-mediated NO production, without affecting cell viability or proliferation. This reduction may be beneficial for patients suffering from periodontitis, an inflammatory disease which results in the destruction of teeth supporting bone and soft tissue. This disease has been associated with elevated levels of NO in the gingival and periodontal tissues.<sup>15-17</sup> Therapies that inhibit NO production may therefore be beneficial, and localized inhibition would be preferable to systemic inhibition, making GTR materials a good candidate for the localized suppression of host-mediated NO signaling.

Modulation of the host response has been proposed as a therapeutic approach for halting tissue destruction associated with periodontitis.<sup>14</sup> Monocytes, when activated, can further differentiate into macrophages, pre-osteoclasts, and osteoclasts, the cells primarily responsible for inflammatory tissue destruction. A GTR membrane that inhibits NO production and reduces monocyte activation may benefit patients with chronic periodontitis undergoing GBR procedures. From our *in vitro* evaluations, improvements are still needed in the tear strength of chitosan membranes before robust clinical applications. Continued efforts are underway to improve the strength and thickness of electrospun chitosan membranes as well as investigating drug loading/release studies to evaluate the potential of electrospun chitosan membranes to act as carrier material for antibiotics and/or growth factors around the graft site.

## CONCLUSION

XRD measurements revealed that crystallinity is decrease upon crosslinking with genipin. *In vitro* biocompatibility testing demonstrated that genipin crosslinking did not have an inhibitory effect on the proliferation of fibroblasts. Electrospun chitosan and genipin-crosslinked electrospun chitosan did not activate RAW 264.7 cells in the absence of LPS. In the presence of LPS, electrospun chitosan and genipin-crosslinked electrospun chitosan mats decreased LPS-induced NO expression in RAW 264.7 monocyte cells. Electrospun chitosan materials demonstrated lower suture pullout strengths than commercially available collagen membranes, even when crosslinked with genipin, demonstrating that improvements are still needed to increase the tear strength before they can successfully be applied as GTR barrier membranes.

## References

1. Kuo SM, Chang SJ, Chen TW, Kuan TC. Guided tissue regeneration for using a chitosan membrane: an experimental study in rats. *J Biomed Mater Res A* 2006;76(2):408-15.
2. Shin SY, Park HN, Kim KH, Lee MH, Choi YS, Park YJ, Lee YM, Ku Y, Rhyu IC, Han SB and others. Biological evaluation of chitosan nanofiber membrane for guided bone regeneration. *J Periodontol* 2005;76(10):1778-84.
3. Yeo YJ, Jeon DW, Kim CS, Choi SH, Cho KS, Lee YK, Kim CK. Effects of chitosan nonwoven membrane on periodontal healing of surgically created one-wall intrabony defects in beagle dogs. *J Biomed Mater Res B Appl Biomater* 2005;72(1):86-93.
4. Sangsanoh P, Supaphol P. Stability improvement of electrospun chitosan nanofibrous membranes in neutral or weak basic aqueous solutions. *Biomacromolecules* 2006;7(10):2710-4.
5. Schiffman JD, Schauer CL. Cross-linking chitosan nanofibers. *Biomacromolecules* 2007a;8(2):594-601.
6. Schiffman JD, Schauer CL. One-step electrospinning of cross-linked chitosan fibers. *Biomacromolecules* 2007b;8(9):2665-7.
7. Khil MS, Cha DI, Kim HY, Kim IS, Bhattarai N. Electrospun nanofibrous polyurethane membrane as wound dressing. *J Biomed Mater Res B Appl Biomater* 2003;67(2):675-9.
8. Rajesh KP, Natarajan TS. Electrospun polymer nanofibrous membrane for filtration. *J Nanosci Nanotechnol* 2009;9(9):5402-5.
9. Subramanian A, Lin HY, Vu D, Larsen G. Synthesis and evaluation of scaffolds prepared from chitosan fibers for potential use in cartilage tissue engineering. *Biomed Sci Instrum* 2004;40:117-22.
10. Wang W, Itoh S, Matsuda A, Ichinose S, Shinomiya K, Hata Y, Tanaka J. Influences of mechanical properties and permeability on chitosan nano/microfiber mesh tubes as a scaffold for nerve regeneration. *J Biomed Mater Res A* 2008;84(2):557-66.

11. Han D, Gouma PI. Electrospun bioscaffolds that mimic the topology of extracellular matrix. *Nanomedicine* 2006;2(1):37-41.
12. Ifkovits JL, Sundararaghavan HG, Burdick JA. Electrospinning fibrous polymer scaffolds for tissue engineering and cell culture. *J Vis Exp* 2009(32).
13. Jang JH, Castano O, Kim HW. Electrospun materials as potential platforms for bone tissue engineering. *Adv Drug Deliv Rev* 2009;61(12):1065-83.
14. Giannobile WV. Host-response therapeutics for periodontal diseases. *J Periodontol* 2008;79(8 Suppl):1592-600.
15. de Sa Siqueira MA, Fischer RG, da Silva Figueredo CM, Brunini TM, Mendes-Ribeiro AC. Nitric oxide and oral diseases: can we talk about it? *Cardiovasc Hematol Agents Med Chem* 2010;8(2):104-12.
16. Ugar-Cankal D, Ozmeric N. A multifaceted molecule, nitric oxide in oral and periodontal diseases. *Clin Chim Acta* 2006;366(1-2):90-100.
17. Daghigh F, Borghaei RC, Thornton RD, Bee JH. Human gingival fibroblasts produce nitric oxide in response to proinflammatory cytokines. *J Periodontol* 2002;73(4):392-400.
18. Yoon HJ, Moon ME, Park HS, Im SY, Kim YH. Chitosan oligosaccharide (COS) inhibits LPS-induced inflammatory effects in RAW 264.7 macrophage cells. *Biochem Biophys Res Commun* 2007;358(3):954-9.
19. Hwang SM, Chen CY, Chen SS, Chen JC. Chitinous materials inhibit nitric oxide production by activated RAW 264.7 macrophages. *Biochem Biophys Res Commun* 2000;271(1):229-33.
20. Madrigal-Carballo S, Rodriguez G, Sibaja M, Reed JD, Vila AO, Molina F. Chitosomes loaded with cranberry proanthocyanidins attenuate the bacterial lipopolysaccharide-induced expression of iNOS and COX-2 in raw 264.7 macrophages. *J Liposome Res* 2009;19(3):189-96.
21. Nam KS, Kim MK, Shon YH. Inhibition of proinflammatory cytokine-induced invasiveness of HT-29 cells by chitosan oligosaccharide. *J Microbiol Biotechnol* 2007;17(12):2042-5.

22. Mi FL, Tan YC, Liang HC, Huang RN, Sung HW. In vitro evaluation of a chitosan membrane cross-linked with genipin. *J Biomater Sci Polym Ed* 2001;12(8):835-50.
23. Mi FL, Tan YC, Liang HF, Sung HW. In vivo biocompatibility and degradability of a novel injectable-chitosan-based implant. *Biomaterials* 2002;23(1):181-91.
24. Chang WH, Chang Y, Lai PH, Sung HW. A genipin-crosslinked gelatin membrane as wound-dressing material: in vitro and in vivo studies. *J Biomater Sci Polym Ed* 2003;14(5):481-95.
25. Focher B, Beltrame PL, Naggi A, Torri G. Alkaline N-deacetylation of chitin enhanced by flash treatments. Reaction kinetics and structure modifications. *Carbohydr Polym* 1990;12:405-418.
26. Rinaudo M, Milas M, Le Dung P. Characterization of Chitosan. Influence of ionic strength and degree of acetylation on chain expansion. *Int J Biol Macromol* 1993;15(5):281-5.
27. Sangsanoh P, Waleetorncheepsawat S, Suwantong O, Wutticharoenmongkol P, Weeranantapan O, Chuenjitbuntaworn B, Cheepsunthorn P, Pavasant P, Supaphol P. In vitro biocompatibility of schwann cells on surfaces of biocompatible polymeric electrospun fibrous and solution-cast film scaffolds. *Biomacromolecules* 2007;8(5):1587-94.
28. Zhang K, Qian Y, Wang H, Fan L, Huang C, Yin A, Mo X. Genipin-crosslinked silk fibroin/hydroxybutyl chitosan nanofibrous scaffolds for tissue-engineering applications. *J Biomed Mater Res Part A* 2010;95(3):870-81.
29. Cho MK, Suh SH, Lee CH, Kim SG. Bovine type I collagen inhibits Raw264.7 cell proliferation through phosphoinositide 3-kinase- and mitogen-activated protein kinase-dependent down-regulation of cyclins D1, A and B1. *Biochim Biophys Acta* 2005;1744(1):47-57.
30. Cho MK, Suh SH, Kim SG. JunB/AP-1 and NF-kappa B-mediated induction of nitric oxide synthase by bovine type I collagen in serum-stimulated murine macrophages. *Nitric Oxide* 2002;6(3):319-32.

31. Tian JY, Sorensen ES, Butler WT, Lopez CA, Sy MS, Desai NK, Denhardt DT. Regulation of no synthesis induced by inflammatory mediators in RAW264.7 cells: collagen prevents inhibition by osteopontin. *Cytokine* 2000;12(5):450-7.
32. Pangestuti R, Bak SS, Kim SK. Attenuation of pro-inflammatory mediators in LPS-stimulated BV2 microglia by chitooligosaccharides via the MAPK signaling pathway. *Int J Biol Macromol* 2011;49(4):599-606.
33. Peluso G, Petillo O, Ranieri M, Santin M, Ambrosio L, Calabro D, Avallone B, Balsamo G. Chitosan-mediated stimulation of macrophage function. *Biomaterials* 1994;15(15):1215-20.
34. Pattani A, Patravale VB, Panicker L, Potdar PD. Immunological effects and membrane interactions of chitosan nanoparticles. *Mol Pharm* 2009;6(2):345-52.
35. Jeong HJ, Koo HN, Oh EY, Chae HJ, Kim HR, Suh SB, Kim CH, Cho KH, Park BR, Park ST and others. Nitric oxide production by high molecular weight water-soluble chitosan via nuclear factor-kappaB activation. *Int J Immunopharmacol* 2000;22(11):923-33.

## CHAPTER 4: Submission to the Journal of Antimicrobial Chemotherapy

### **Antimicrobial activity of minocycline-loaded genipin-crosslinked nano-fibrous chitosan mats for guided tissue regeneration.**

Authors: Norowski, PA, Babu, J, Adatrow, PC, Haggard, WO, Bumgardner, JD.

#### **Abstract**

Antimicrobial delivery has been advocated for guided tissue regeneration (GTR) or guided bone regeneration (GBR) therapies involving patients with aggressive or unresolved periodontitis/peri-implantitis. Electrospun chitosan membranes demonstrate several advantages over traditional GTR barrier membranes because they stimulate healing, mimic the topology of the extracellular matrix, and allow for diffusion of nutrients and wastes into/out of the graft site, and were shown to stimulate bone formation in a rabbit calvarial critical-size defect model. Previously, we have shown improvements in mechanical properties and degradation kinetics by crosslinking electrospun membranes with 5 mM or 10 mM genipin. We have also previously demonstrated the ability of electrospun chitosan membranes to inhibit lipopolysaccharide (LPS)-induced monocyte activation. In this study, minocycline was incorporated into the chitosan membrane by passive absorption at 5 or 10 mg/mL. The minocycline-loaded membranes and control membranes (carrier only) were tested against *Porphyromonas gingivalis* (*P. gingivalis*) by repeated zone of inhibition measurements. Results show that uncrosslinked and genipin-crosslinked membranes have similar capacity to absorb aqueous solutions. Minocycline loading resulted in bacterial inhibition for up to 8 days from crosslinked membranes whereas uncrosslinked membranes loaded with minocycline only inhibited bacteria for 4 days. These *in vitro* results suggest that genipin-crosslinked

electrospun chitosan membranes loaded with minocycline may be able to reduce early bacterial contamination of GTR graft sites.

## **Introduction**

Electrospun chitosan and other chitosan membrane materials have been advocated for guided bone regeneration (GBR) and guided tissue regeneration (GTR) barrier membranes.<sup>1-3</sup> Electrospun material are advantageous because they mimic the topology of the extracellular matrix<sup>4</sup>, allow the diffusion of nutrients and waste, while having a small enough pore size to limit cellular infiltration. Electrospun materials also have the capability to regenerate dense cortical bone in animal models.<sup>5</sup>

Chitosan is advantageous because it has been reported to stimulate the healing of dental pulp wounds,<sup>6</sup> is osteogenic,<sup>7</sup> and has been shown to inhibit lipopolysaccharide (LPS)-induced monocyte activation.<sup>8-11</sup> However, improvements are needed in the clinical handle-ability, strength, and degradation timeframe of electrospun chitosan for clinical GTR applications. We have shown previously that crosslinking electrospun chitosan membranes with genipin resulted in 12% reduction in mass loss over 16 weeks, and increased the tensile strength of the membranes three fold [Norowski et al., in review]. We have also demonstrated that the genipin crosslinked chitosan membranes were not cytotoxic to osteoblast or fibroblast cells, and did not cause monocyte activation. Electrospun chitosan material may have the capacity to deliver antimicrobials, such as minocycline, during GTR regeneration of periodontal lesions in a manner similar to Arestin® (OraPharma, Warminster PA, USA) which is used for the extended local delivery of minocycline to periodontal pockets.<sup>12</sup> This product consists of

microencapsulated minocycline in which the microcapsules are composed of PLGA synthetic co-polymer.

Periodontitis is an inflammatory disease that is driven by the presence of gram-negative periopathogens in the gingival tissues. These pathogens secrete LPS, a potent inflammatory molecule, which drives host inflammatory response. Monocytes, activated macrophages and polymorphonuclear leukocytes (PMNs) respond to secreted LPS by participating in paracrine and autocrine signaling amplification using NO, IL-1 $\beta$  and TNF- $\alpha$  among a myriad of other cytokines.<sup>13</sup> Ultimately these signaling cascades lead to the recruitment of cells that release tissue destroying enzymes, namely collagenase, MMP-2, MMP-8, MMP-9 among others. Therapeutics that have the ability to inhibit MMPs or inflammatory cell activation may potentially limit tissue and bone destruction associated with periodontitis and other inflammatory diseases.<sup>14</sup> Previously, we have shown the ability of genipin crosslinked electrospun chitosan membranes to inhibit the LPS-induced release of NO from RAW 264.7 monocyte cells over a 3 day period [Norowski, in review]. NO expression is elevated in the periodontal and gingival tissues of patients with periodontitis and its inhibition is a potential therapeutic target.<sup>15-17</sup> Minocycline is commonly used in periodontal therapy as an antimicrobial agent but it also has the ability to limit tissue destruction, by inhibition of tissue destroying enzymes such as collagenase, MMP-2 and MMP-9.<sup>18</sup>

In this study, uncrosslinked and genipin crosslinked electrospun chitosan membranes were impregnated by immersion in 10 mg/mL minocycline or 5 mg/mL minocycline and tested against *Porphyromonas gingivalis* (*P. gingivalis*) by zone of inhibition. *P. gingivalis* is an important and extensively studied periodontal pathogen

involved in the pathogenesis of periodontitis. In addition, swelling was measured to assess the capacity of the electrospun membranes to absorb aqueous solutions.

## **Materials and Methods**

### **Electrospinning procedure**

Electrospun chitosan nanofibrous mats were fabricated as previously described [Norowski et al., in review]. Briefly, a 5.50wt% chitosan solution in 70(v/v)% trifluoroacetic acid and 30(v/v)% methylene chloride was mixed with genipin for 30 minutes prior to the start of electrospinning. The genipin concentrations investigated were 0, 5, or 10 mM. The solution was electrospun at 25 kV and the fibers were collected on a non-stick aluminum foil target, rotated at 8.4 RPM by an AC motor to ensure even and random distribution of fibers. After electrospinning, the nano-fibrous mat was put under vacuum overnight to remove residual solvent, removed from the foil, and then neutralized at room temperature in 5M Na<sub>2</sub>CO<sub>3</sub> (saturated solution) for 3 hours.<sup>19</sup> Membranes were sterilized by ethylene oxide gas.

### **Swelling**

The swelling index of the nanofibrous membranes was determined by a swelling test. Swelling in phosphate buffered saline (PBS) was evaluated to estimate the amount of antibiotic solution that could be absorbed by the electrospun membranes. To determine the dry weight, membranes were maintained at 40 °C overnight in a drying oven. After measuring the dry weight, membranes were submerged in PBS for 1 hr (±15 minutes) to ensure complete swelling. Swelling index was calculated by  $(W_{t_{WET}} - W_{t_{DRY}})/W_{t_{DRY}}$ .

### **Minocycline loading**

Minocycline was loaded into chitosan nano-fibrous membranes by passive absorption. Pre-cut, pre-sterilized circular specimens (10 mm diameter), were submersed in minocycline solution (10 or 5 mg/mL in de-ionized water) for 15 minutes. Negative

controls were submersed in de-ionized water only. Minocycline solutions were weighed before and after membrane swelling to determine the amount of antibiotic solution absorbed.

***P. gingivalis* Zone of Inhibition (ZOI)**

The model periodontal pathogen used in this study was *Porphyromonas gingivalis* (ATCC No 33277) which was originally isolated from human gingival sulcus. Bacteria were maintained as frozen stock cultures and grown anaerobically at 37°C in trypticase soy broth (BD BBL, Franklin Lakes, NJ, USA) supplemented with 1 g of yeast extract per liter, 5 mg of hemin per liter, and 1 mg of menadione per liter. After 72 hours of growth, bacteria were collected and resuspended to contain  $1 \times 10^7$  cells/ml. A suspension (0.5 ml) of this stock suspension was spread on a blood agar plate (BD BBL, Franklin Lakes, NJ, USA) and the electrospun chitosan mats loaded with minocycline were placed onto the agar and incubated in an anaerobic jar with an anaerobic pack. Plates were checked for ZOI by serially placing membranes on freshly seeded bacterial lawns and recording ZOI at days 1, 4, 6, 8 and 11 (n=2).

## Results

Swelling experiments demonstrated that the electrospun membranes have a swelling ratio around 2.0 (Figure 1). The amount of swelling that occurred was not significantly affected by crosslinking ( $p=0.29$ ). Although swelling was allowed to occur for 1 hour to ensure complete swelling, the membranes appeared to be fully hydrated within 5 minutes (data not shown). Submersion in 10 mg/mL minocycline solution resulted in 0.52, 0.53, and 0.38 mg of minocycline uptake for uncrosslinked, 5 mM crosslinked and 10 mM genipin-crosslinked membranes, respectively.

Bacterial ZOI testing demonstrated extended release of minocycline from the barrier membrane *in vitro* for up to 8 days after soaking in 10 mg/mL (figure 2) or 5 mg/mL (figure 3) minocycline for 15 minutes. It was noted that uncrosslinked membranes only remained bacteriostatic for 4 days as opposed to both levels of crosslinking which remained bacteriostatic for 8 days. None of the negative controls (carrier only) produced zones of inhibition.

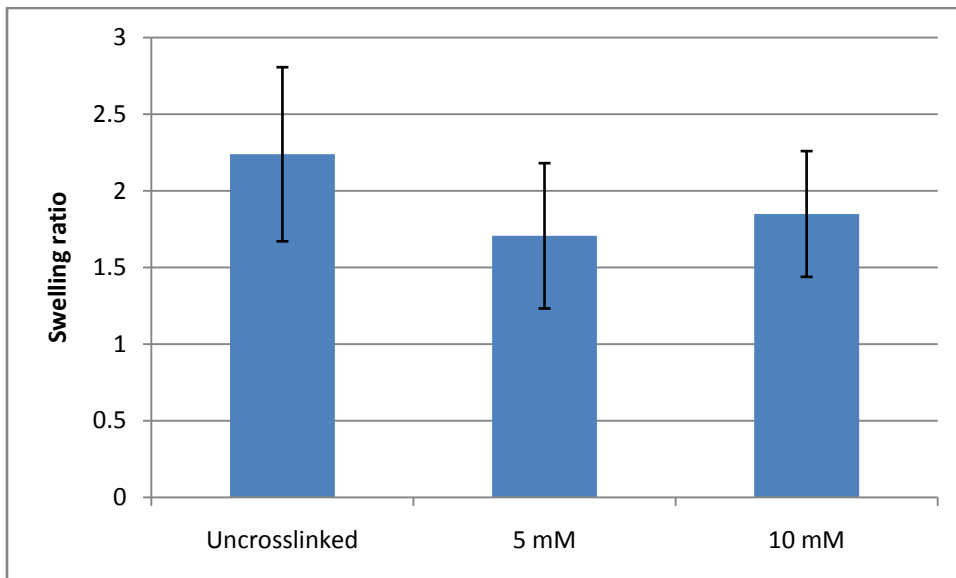


**Figure 1 – Swelling ratio of the nanofibrous chitosan mats. There were no significant differences between groups ( $p=0.29$ ,  $n=4$ ,  $*n=5$  in 5 mM group)**

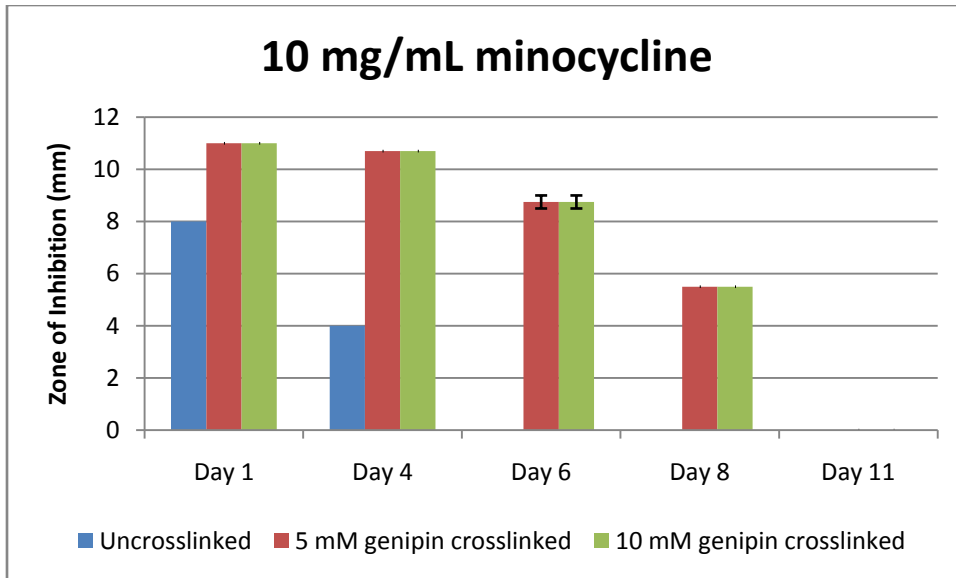


**Figure 2 – Inhibition of *P. gingivalis* over an 11 day period by electrospun chitosan membrane loaded with 10 mg/mL minocycline. Error bars represent the spread of measurements (n=2).**

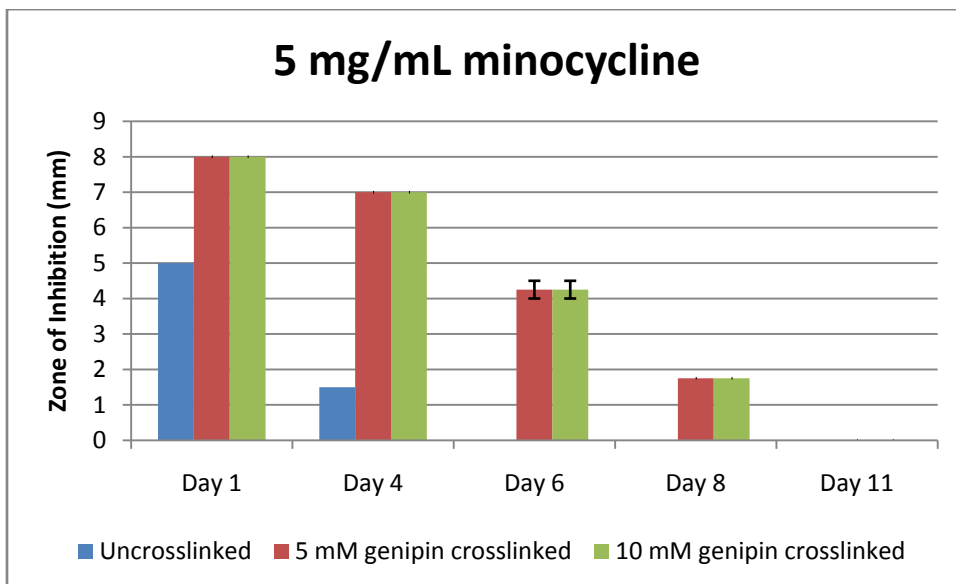


**Figure 3 – Inhibition of *P. gingivalis* over an 11 day period by electrospun chitosan membrane loaded with 5 mg/mL minocycline. Error bars represent the spread of measurements (n=2).**

## Discussion

The slightly reduced swelling experienced by crosslinked membranes may have been caused by decreased chain packing and restricted chain movement. Since the membranes absorb comparable amounts of fluid and the slight reduction in swelling was not significant, the crosslinked membrane should have similar capacity to absorb drugs, antibiotics, or growth factor solutions. Unlike vapor crosslinking and solution crosslinking, where materials are exposed to a crosslinking agent which crosslinks the surface of the material only, in this study, the crosslinking agent is dispersed within the polymer solution used for scaffold fabrication. This situation creates a more uniformly and thoroughly crosslinked membrane, which may contribute to antibiotic retention and more uniform degradation kinetics. A previous examination using x-ray diffraction showed that crystallinity was decreased during crosslinking. This may have contributed to slightly lower swelling volumes, however this difference was not significant, and the amount of minocycline loaded into the membranes was comparable.

In this study, genipin-crosslinked electrospun chitosan was able to absorb minocycline and release it in an extended manner that remained bacteriostatic for longer periods than uncrosslinked membranes (8 days as compared to 4 days). These results are similar to reports by others who have loaded biodegradable GTR membranes with antibiotics/antiseptics such as tetracycline, doxycycline or chlorhexidine.<sup>20-22</sup> The delayed degradation kinetics [Norowski et al., in review] contributed to the extended release seen from crosslinked membranes. Thus, uncrosslinked chitosan membranes degraded faster, and resulted in a faster burst release of minocycline.

One clinical investigation reported no improvements in clinical parameters associated with the local application of minocycline ointment before GTR therapy, but this study did not investigate minocycline incorporation into the GTR membrane itself, and only investigated the use of type 1 collagen membranes.<sup>23</sup> Other investigations with a non-membrane local delivery system demonstrated improvement in clinical parameters associated with the use of minocycline microcapsules (Arestin®).<sup>12</sup> This microcapsule study also showed that reduction in periodontal pocket probing depth (improved clinical outcomes) correlated strongly with the ability to inhibit red complex bacteria *in vitro*, a sub-group of periodontal pathogens that includes *P. gingivalis*, *T. forsythia*, and *T. denticola*.<sup>12</sup> This correlation strongly suggests that minocycline-loaded genipin-crosslinked electrospun chitosan mats could be beneficial to patients with unresolved periodontitis undergoing GTR surgery, since they inhibited *P. gingivalis*, a red-complex bacteria, *in vitro*.

## **Conclusion**

In this study, we have shown the ability of genipin-crosslinked electrospun chitosan to deliver clinically relevant levels of minocycline over an 8 day period. The eluted minocycline was able to inhibit growth of *P. gingivalis*, a model periopathogen, *in vitro*. Crosslinked membranes released inhibitory concentrations of minocycline for 8 days while, uncrosslinked membranes only inhibited growth for 4 days. This prolonged minocycline elution profile suggests that genipin-crosslinking improved the drug-carrier properties of electrospun chitosan.

## References

1. Kuo SM, Chang SJ, Chen TW et al. Guided tissue regeneration for using a chitosan membrane: an experimental study in rats. *Journal of biomedical materials research* 2006; **76**: 408-15.
2. Shin SY, Park HN, Kim KH et al. Biological evaluation of chitosan nanofiber membrane for guided bone regeneration. *Journal of periodontology* 2005; **76**: 1778-84.
3. Yeo YJ, Jeon DW, Kim CS et al. Effects of chitosan nonwoven membrane on periodontal healing of surgically created one-wall intrabony defects in beagle dogs. *J Biomed Mater Res B Appl Biomater* 2005; **72**: 86-93.
4. Chen F, Li X, Mo X et al. Electrospun chitosan-P(LLA-CL) nanofibers for biomimetic extracellular matrix. *Journal of biomaterials science* 2008; **19**: 677-91.
5. Cai YZ, Wang LL, Cai HX et al. Electrospun nanofibrous matrix improves the regeneration of dense cortical bone. *J Biomed Mater Res A* 2010; **95**: 49-57.
6. Matsunaga T, Yanagiguchi K, Yamada S et al. Chitosan Monomer promotes tissue regeneration on dental pulp wounds. *J Biomed Mater Res A* 2005; **76**: 711-20.
7. Khor E, Lim YL. Implantable applications of chitin and chitosan. *Biomaterials* 2003; **24**: 2339-49.
8. Yoon HJ, Moon ME, Park HS et al. Chitosan oligosaccharide (COS) inhibits LPS-induced inflammatory effects in RAW 264.7 macrophage cells. *Biochemical and biophysical research communications* 2007; **358**: 954-9.
9. Hwang SM, Chen CY, Chen SS et al. Chitinous materials inhibit nitric oxide production by activated RAW 264.7 macrophages. *Biochemical and biophysical research communications* 2000; **271**: 229-33.
10. Madrigal-Carballo S, Rodriguez G, Sibaja M et al. Chitosomes loaded with cranberry proanthocyanidins attenuate the bacterial lipopolysaccharide-induced expression of iNOS and COX-2 in raw 264.7 macrophages. *Journal of liposome research* 2009; **19**: 189-96.

11. Nam KS, Kim MK, Shon YH. Inhibition of proinflammatory cytokine-induced invasiveness of HT-29 cells by chitosan oligosaccharide. *Journal of microbiology and biotechnology* 2007; **17**: 2042-5.
12. Bland P, Goodson J, Gunsolley J et al. Association of antimicrobial and clinical efficacy: periodontitis therapy with minocycline microspheres. *J Int Acad Periodontol* 2010; **12**: 11-9.
13. Deo V, Bhongade ML. Pathogenesis of periodontitis: role of cytokines in host response. *Dentistry today* 2010; **29**: 60-2, 4-6; quiz 8-9.
14. Giannobile WV. Host-response therapeutics for periodontal diseases. *J Periodontol* 2008; **79**: 1592-600.
15. de Sa Siqueira MA, Fischer RG, da Silva Figueredo CM et al. Nitric oxide and oral diseases: can we talk about it? *Cardiovascular & hematological agents in medicinal chemistry* 2010; **8**: 104-12.
16. Ugar-Cankal D, Ozmeric N. A multifaceted molecule, nitric oxide in oral and periodontal diseases. *Clinica chimica acta; international journal of clinical chemistry* 2006; **366**: 90-100.
17. Daghigh F, Borghaei RC, Thornton RD et al. Human gingival fibroblasts produce nitric oxide in response to proinflammatory cytokines. *J Periodontol* 2002; **73**: 392-400.
18. Rifkin BR, Vernillo AT, Golub LM. Blocking periodontal disease progression by inhibiting tissue-destructive enzymes: a potential therapeutic role for tetracyclines and their chemically-modified analogs. *J Periodontol* 1993; **64**: 819-27.
19. Sangsanoh P, Supaphol P. Stability improvement of electrospun chitosan nanofibrous membranes in neutral or weak basic aqueous solutions. *Biomacromolecules* 2006; **7**: 2710-4.
20. Chang CY, Yamada S. Evaluation of the regenerative effect of a 25% doxycycline-loaded biodegradable membrane for guided tissue regeneration. *J Periodontol* 2000; **71**: 1086-93.

21. Chen YT, Hung SL, Lin LW et al. Attachment of periodontal ligament cells to chlorhexidine-loaded guided tissue regeneration membranes. *J Periodontol* 2003; **74**: 1652-9.
  
22. Park YJ, Lee YM, Park SN et al. Enhanced guided bone regeneration by controlled tetracycline release from poly(L-lactide) barrier membranes. *J Biomed Mater Res* 2000; **51**: 391-7.
  
23. Minabe M, Kodama T, Kogou T et al. Clinical significance of antibiotic therapy in guided tissue regeneration with a resorbable membrane. *Periodontal Clin Investig* 2001; **23**: 20-30.

## Chapter 5. Conclusions

In this study, the design criteria for the chitosan based GTR membrane was to be able to exclude the soft tissue (i.e. cell occlusive), to degrade on a time scale consistent with healing and osseous tissue maturation, to provide a topology and nanostructure that supports cell attachment/tissue integration, to provide bioactivity by stimulating wound healing and osseous regeneration through the inherent properties of chitosan, or through the delivery of some bioactive compound. To meet the design criteria, three GTR barrier membranes formulations were fabricated from chitosan by electrospinning, and chemically modified by incorporation of genipin at 5 mM or 10 mM concentrations during the electrospinning process. These electrospun chitosan membranes and crosslinked membranes were evaluated *in vitro* for their capacity to perform as a GTR barrier membrane. Chitosan membranes were evaluated to act as carriers for local delivery of the periodontal antibiotic, minocycline. Minocycline is also beneficial to patients with periodontitis because it is a collagenase and MMP inhibitor [65, 66], thus limiting tissue destruction and gingival recession associated with periodontitis.

Results from the XRD, FTIR, as well as physical changes in, color, rigidity, are evidence that chemical crosslinking occurred during genipin incorporation. Specifically, results from FTIR analysis showed a dose dependent reduction in the amount of free amino groups, indicating that genipin was binding the amino groups during crosslinking. We also demonstrated by SEM imaging that the mean fiber diameter was not significantly affected by crosslinking. Additionally, altered *in vitro* biodegradation was observed, with crosslinking causing a 12% delay in mass loss over a 16 week period. However, the bioactive properties and biocompatibility of the membranes was not

affected by genipin-crosslinking in cultures of osteoblasts, fibroblasts, and monocyte cells. Tensile strength was also significantly increased by 265% with 10 mM genipin crosslinking, but suture pullout strength was increased by only 44% which was not significant. Increases in mechanical strength appeared to be genipin-dose dependent. These results suggest that genipin-crosslinking benefits the tensile properties and improves the handling characteristics of the membranes, but does not particularly benefit the tear strength of the membrane which is more indicative of clinical performance when the membrane is sutured. The tear strength of electrospun chitosan membranes must be improved for clinical application, because it was significantly lower than that of BioMend Extend (Zimmer Dental, Carlsbad, CA). This improvement could be achieved by increasing the thickness of the electrospun mats, or by increasing fiber entanglement/adhesion and/or decreasing the amount of bead defects.

XRD showed that electrospun membranes were more crystalline without crosslinking. The reduction in crystallinity was from 37 % crystallinity index, to 20 % crystallinity index, which was statistically significant. Importantly, the reduction in crystallinity did not significantly affect the swelling capabilities of the crosslinked membrane. Swelling tests of the membranes demonstrated little or no difference in saline uptake with crosslinking, indicating that crosslinked membranes could be loaded with antimicrobials or growth factors in a manner similar to uncrosslinked membranes. When submersed in a solution of 10 or 5 mg/mL minocycline the genipin-crosslinked membranes provided an extended antimicrobial action against model periodontal pathogen *P. gingivalis* for up to 8 days as compared to only 4 days for uncrosslinked. This duration of antimicrobial action should be sufficient to allow primary soft tissue

healing and attachment in the absence of periodontal pathogens. Furthermore, minocycline also has the ability to inhibit collagenase and certain MMPs [27, 65, 66], indicating that minocycline loaded chitosan membranes could potentially provide extended bone and soft tissue-sparing bioactivities.

The results of this investigation have shown that genipin-crosslinked electrospun chitosan mats have beneficial biological properties including cytocompatibility, the ability to inhibit LPS-induced monocyte activation, and the ability to deliver minocycline over an 8 day period which offers clinical advantage over current collagen membranes. However, improvements in the shear strength and clinical handle-ability of electrospun chitosan mats are still needed.

## Chapter 6. Recommendations

The genipin-crosslinked electrospun chitosan mats are a promising material for GTR barrier membrane implants. These *in vitro* investigations on the genipin-crosslinked electrospun chitosan have shown that improvements are needed in the tear strength of the material. One approach for a more rapid development would be to not develop electrospun chitosan as a stand-alone GTR membrane, which would require the engineering of electrospun materials to obtain optimal mechanical strength and degradation kinetics. Instead, the application of electrospinning technology to already clinically-used collagen membranes would result in a bi-layer composite construct. The bi-layer construct can easily be accomplished by directly electrospinning chitosan onto a collagen membrane substrate. This approach would result in a bioactive surface, which could promote cell attachment and reduce LPS-induced monocyte activation but would also have the beneficial handling properties of collagen membranes that clinicians prefer and are familiar with.

Another recommendation is to increase the thickness of the resultant membrane to increase mechanical properties and improve handling characteristics of the membrane. This could be accomplished by increasing the efficiency of the electrospinning process, by allowing less material to be lost during the spinning process. It could also be accomplished by decreasing the target size, which would result in a smaller, but thicker, membrane.

Investigations into the *in vivo* general biocompatibility are necessary to confirm tissue compatibility and *in vivo* degradation timeframe. A good model for this would be the Sprague-Dawley rat intramuscular pouch model. The next logical step, after

demonstrating basic tissue compatibility, would be to use a pre-clinical animal model to evaluate under conditions of intended use the potential of minocycline-loaded genipin-crosslinked electrospun chitosan membranes to inhibit chronic periodontitis. One possible model is the LPS-induced osteolysis model of aggressive periodontitis used to evaluate potential bone sparing therapies [44]. In this model, Sprague-Dawley rats are given palatal molar gingival injections of LPS derived from *Actinobacillus actinomycetemcomitans* three times per week for 8 weeks. At 8 weeks, alveolar bone loss is measured by  $\mu$ CT [44]. This would represent a worst-case scenario and would be a challenging model to establish efficacy of minocycline-loaded genipin-crosslinked electrospun chitosan membranes to inhibit/reduce tissue destruction associated with aggressive/chronic periodontitis. However, this animal model does not fully capture the etiology and pathogenesis of periodontitis, because it doesn't cause bone loss from pathogenic dental plaque but from direct injection of LPS into the gingival tissues.

The most appropriate (and more expensive) animal model for periodontitis would be ligature-induced bone loss model in non-human primates [67]. In this model, bony defects are created around teeth using wire ligatures are positioned to extend from the oral cavity into the defect space. This model allows for plaque accumulation on the wire ligature and results in chronic inflammation, leading to bone loss. After a bone loss has occurred, the ligatures are removed and experimental materials can be applied. Often a small notch is placed in the root of the tooth to mark the original defect depth, and so that measurements can later be obtained. Histological measurements are taken to examine the height of regeneration which has occurred from the base of the tooth notch to the most coronal extension of bone, periodontal ligament, and cementum tissues [67]. This pre-

clinical model most closely approximates the clinical manifestations of periodontitis in humans, and would be the best method to evaluate potential therapies.

## Chapter 7. References

1. Retzepe M, Donos N (2010) Guided Bone Regeneration: biological principle and therapeutic applications. *Clin Oral Implants Res* 21(6):567-76
2. Kaufman E, Wang PD (2003) Localized vertical maxillary ridge augmentation using symphyseal bone cores: a technique and case report. *Int J Oral Maxillofac Implants* 18(2):293-8
3. McAllister BS, Haghghat K (2007) Bone augmentation techniques. *J Periodontol* 78(3):377-96
4. Iatrou I, Theologie-Lygidakis N, Angelopoulos A (2001) Use of membrane and bone grafts in the reconstruction of orbital fractures. *Oral Surg Oral Med Oral Pathol Oral Radiol Endod* 91(3):281-6
5. Scott JK, Webb RM, Flood TR (2007) Premaxillary osteotomy and guided tissue regeneration in secondary bone grafting in children with bilateral cleft lip and palate. *Cleft Palate Craniofac J* 44(5):469-75
6. Testori T, Wallace SS, Del Fabbro M, Taschieri S, Trisi P, Capelli M, Weinstein RL (2008) Repair of large sinus membrane perforations using stabilized collagen barrier membranes: surgical techniques with histologic and radiographic evidence of success. *Int J Periodontics Restorative Dent* 28(1):9-17
7. Bhumbra RP, Walker PS, Berman AB, Emmanuel J, Barrett DS, Blunn GW (2000) Prevention of loosening in total hip replacements using guided bone regeneration. *Clin Orthop Relat Res*(372):192-204
8. Guo X, Guo H, Liu J (1998) [Membrane guided tissue regeneration in the treatment of bone defect]. *Zhongguo Xiu Fu Chong Jian Wai Ke Za Zhi* 12(5):301-3
9. Roos-Jansaker AM, Renvert S, Egelberg J (2003) Treatment of peri-implant infections: a literature review. *J Clin Periodontol* 30(6):467-85
10. Park YJ, Lee YM, Park SN, Lee JY, Ku Y, Chung CP, Lee SJ (2000) Enhanced guided bone regeneration by controlled tetracycline release from poly(L-lactide) barrier membranes. *J Biomed Mater Res* 51(3):391-7

11. Schou S, Berglundh T, Lang NP (2004) Surgical treatment of peri-implantitis. *Int J Oral Maxillofac Implants* 19 Suppl:140-9
12. Roos-Jansaker AM, Renvert H, Lindahl C, Renvert S (2007) Surgical treatment of peri-implantitis using a bone substitute with or without a resorbable membrane: a prospective cohort study. *J Clin Periodontol* 34(7):625-32
13. Zybutz MD, Laurell L, Rapoport DA, Persson GR (2000) Treatment of intrabony defects with resorbable materials, non-resorbable materials and flap debridement. *J Clin Periodontol* 27(3):169-78
14. Becker W, Dahlin C, Becker BE, Lekholm U, van Steenberghe D, Higuchi K, Kultje C (1994) The use of e-PTFE barrier membranes for bone promotion around titanium implants placed into extraction sockets: a prospective multicenter study. *Int J Oral Maxillofac Implants* 9(1):31-40
15. Needleman IG, Worthington HV, Giedrys-Leeper E, Tucker RJ (2006) Guided tissue regeneration for periodontal infra-bony defects. *Cochrane Database Syst Rev*(2):CD001724
16. Needleman I, Tucker R, Giedrys-Leeper E, Worthington H (2005) Guided tissue regeneration for periodontal intrabony defects--a Cochrane Systematic Review. *Periodontol* 2000 37:106-23
17. Powell CA, Mealey BL, Deas DE, McDonnell HT, Moritz AJ (2005) Post-surgical infections: prevalence associated with various periodontal surgical procedures. *J Periodontol* 76(3):329-33
18. Sculean A, Nikolidakis D, Schwarz F (2008) Regeneration of periodontal tissues: combinations of barrier membranes and grafting materials - biological foundation and preclinical evidence: a systematic review. *J Clin Periodontol* 35(8 Suppl):106-16
19. Novaes AB, Jr., Palioto DB, de Andrade PF, Marchesan JT (2005) Regeneration of class II furcation defects: determinants of increased success. *Braz Dent J* 16(2):87-97
20. Murphy KG, Gunsolley JC (2003) Guided tissue regeneration for the treatment of periodontal intrabony and furcation defects. A systematic review. *Ann Periodontol* 8(1):266-302

21. Gottlow J, Nyman S (1996) Barrier membranes in the treatment of periodontal defects. *Curr Opin Periodontol* 3:140-8
22. Albandar JM (2002) Periodontal diseases in North America. *Periodontol* 2000 29:31-69
23. de Sa Siqueira MA, Fischer RG, da Silva Figueredo CM, Brunini TM, Mendes-Ribeiro AC (2010) Nitric oxide and oral diseases: can we talk about it? *Cardiovasc Hematol Agents Med Chem* 8(2):104-12
24. Giannobile WV (2008) Host-response therapeutics for periodontal diseases. *J Periodontol* 79(8 Suppl):1592-600
25. Lindhe J, Westfelt E, Nyman S, Socransky SS, Haffajee AD (1984) Long-term effect of surgical/non-surgical treatment of periodontal disease. *J Clin Periodontol* 11(7):448-58
26. Lindhe J, Socransky SS, Nyman S, Haffajee A, Westfelt E (1982) "Critical probing depths" in periodontal therapy. *J Clin Periodontol* 9(4):323-36
27. Chang KM, Ryan ME, Golub LM, Ramamurthy NS, McNamara TF (1996) Local and systemic factors in periodontal disease increase matrix-degrading enzyme activities in rat gingiva: effect of micocycline therapy. *Res Commun Mol Pathol Pharmacol* 91(3):303-18
28. Ito K, Nanba K, Murai S (1998) Effects of bioabsorbable and non-resorbable barrier membranes on bone augmentation in rabbit calvaria. *J Periodontol* 69(11):1229-37
29. Simion M, Scarano A, Gionso L, Piattelli A (1996) Guided bone regeneration using resorbable and nonresorbable membranes: a comparative histologic study in humans. *Int J Oral Maxillofac Implants* 11(6):735-42
30. Bohning BP, Davenport WD, Jeanson BG (1999) The effect of guided tissue regeneration on the healing of osseous defects in rat calvaria. *J Endod* 25(2):81-4
31. Moses O, Vitrial D, Aboodi G, Sculean A, Tal H, Kozlovsky A, Artzi Z, Weinreb M, Nemcovsky CE (2008) Biodegradation of three different collagen membranes in the rat calvarium: a comparative study. *J Periodontol* 79(5):905-11

32. Tal H, Kozlovsky A, Artzi Z, Nemcovsky CE, Moses O (2008) Long-term biodegradation of cross-linked and non-cross-linked collagen barriers in human guided bone regeneration. *Clin Oral Implants Res* 19(3):295-302
33. Clarizio LF (1999) Successful implant restoration without the use of membrane barriers. *J Oral Maxillofac Surg* 57(9):1117-21
34. Bornstein MM, Bosshardt D, Buser D (2007) Effect of two different bioabsorbable collagen membranes on guided bone regeneration: a comparative histomorphometric study in the dog mandible. *J Periodontol* 78(10):1943-53
35. Schliephake H, Dard M, Planck H, Hierlemann H, Jakob A (2000) Guided bone regeneration around endosseous implants using a resorbable membrane vs a PTFE membrane. *Clin Oral Implants Res* 11(3):230-41
36. Liu H, Slamovich EB, Webster TJ (2006) Less harmful acidic degradation of poly(lactico-glycolic acid) bone tissue engineering scaffolds through titania nanoparticle addition. *Int J Nanomedicine* 1(4):541-5
37. Christgau M, Bader N, Schmalz G, Hiller KA, Wenzel A (1997) Postoperative exposure of bioresorbable GTR membranes: effect on healing results. *Clin Oral Investig* 1(3):109-18
38. De Sanctis M, Zucchelli G, Clauser C (1996) Bacterial colonization of bioabsorbable barrier material and periodontal regeneration. *J Periodontol* 67(11):1193-200
39. Scott TA, Towle HJ, Assad DA, Nicoll BK (1997) Comparison of bioabsorbable laminar bone membrane and non-resorbable ePTFE membrane in mandibular furcations. *J Periodontol* 68(7):679-86
40. Urbani G, Graziani A, Lombardo G, Caton JG (1997) Clinical results with exposed polyglactin 910 resorbable membranes for guided tissue regeneration. *Int J Periodontics Restorative Dent* 17(1):41-51
41. Nowzari H, London R, Slots J (1995) The importance of periodontal pathogens in guided periodontal tissue regeneration and guided bone regeneration. *Compend Contin Educ Dent* 16(10):1042, 1044, 1046 passim; quiz 1058

42. Thomas MV, Puleo DA (2011) Infection, inflammation, and bone regeneration: a paradoxical relationship. *J Dent Res* 90(9):1052-61
43. Deo V, Bhongade ML (2010) Pathogenesis of periodontitis: role of cytokines in host response. *Dent Today* 29(9):60-2, 64-6; quiz 68-9
44. Rogers JE, Li F, Coatney DD, Rossa C, Bronson P, Krieder JM, Giannobile WV, Kirkwood KL (2007) Actinobacillus actinomycetemcomitans lipopolysaccharide-mediated experimental bone loss model for aggressive periodontitis. *J Periodontol* 78(3):550-8
45. Minabe M, Kodama T, Kogou T, Fushimi H, Sugiyama T, Takeuchi K, Miterai E, Nishikubo S (2001) Clinical significance of antibiotic therapy in guided tissue regeneration with a resorbable membrane. *Periodontal Clin Investig* 23(1):20-30
46. Ugar-Cankal D, Ozmeric N (2006) A multifaceted molecule, nitric oxide in oral and periodontal diseases. *Clin Chim Acta* 366(1-2):90-100
47. Khor E, Lim YL (2003) Implantable applications of chitin and chitosan. *Biomaterials* 24:2339-2349
48. Di Martino A, Sittinger M, Risbud MV (2005) Chitosan: a versatile biopolymer for orthopaedic tissue-engineering. *Biomaterials* 26(30):5983-90
49. Kuo SM, Chang SJ, Chen TW, Kuan TC (2006) Guided tissue regeneration for using a chitosan membrane: an experimental study in rats. *J Biomed Mater Res A* 76(2):408-15
50. Yeo YJ, Jeon DW, Kim CS, Choi SH, Cho KS, Lee YK, Kim CK (2005) Effects of chitosan nonwoven membrane on periodontal healing of surgically created one-wall intrabony defects in beagle dogs. *J Biomed Mater Res B Appl Biomater* 72(1):86-93
51. Baker BM, Gee AO, Metter RB, Nathan AS, Marklein RA, Burdick JA, Mauck RL (2008) The potential to improve cell infiltration in composite fiber-aligned electrospun scaffolds by the selective removal of sacrificial fibers. *Biomaterials* 29(15):2348-58

52. Kim KH, Jeong L, Park HN, Shin SY, Park WH, Lee SC, Kim TI, Park YJ, Seol YJ, Lee YM, Ku Y, Rhyu IC, Han SB, Chung CP (2005) Biological efficacy of silk fibroin nanofiber membranes for guided bone regeneration. *J Biotechnol* 120(3):327-39
53. Liao S, Li B, Ma Z, Wei H, Chan C, Ramakrishna S (2006) Biomimetic electrospun nanofibers for tissue regeneration. *Biomed Mater* 1(3):R45-53
54. Jin Q, Wei G, Lin Z, Sugai JV, Lynch SE, Ma PX, Giannobile WV (2008) Nanofibrous scaffolds incorporating PDGF-BB microspheres induce chemokine expression and tissue neogenesis in vivo. *PLoS One* 3(3):e1729
55. Koga T, Kitamura K, Higashi N (2009) Stimuli-responsive peptide self-assembly into well-organized nanofibers. *Adv Exp Med Biol* 611:237-8
56. Schneider A, Garlick JA, Egles C (2008) Self-assembling peptide nanofiber scaffolds accelerate wound healing. *PLoS One* 3(1):e1410
57. Vasita R, Katti DS (2006) Nanofibers and their applications in tissue engineering. *Int J Nanomedicine* 1(1):15-30
58. Sill TJ, von Recum HA (2008) Electrospinning: applications in drug delivery and tissue engineering. *Biomaterials* 29(13):1989-2006
59. Pham QP, Sharma U, Mikos AG (2006) Electrospinning of polymeric nanofibers for tissue engineering applications: a review. *Tissue Eng* 12(5):1197-211
60. Ohkawa K, Cha D, Kim H, Nishida A, Yamamoto H (2004) Electrospinning of Chitosan. *Macromol Rapid Commun* 25:1600-1605
61. Cai YZ, Wang LL, Cai HX, Qi YY, Zou XH, Ouyang HW (2010) Electrospun nanofibrous matrix improves the regeneration of dense cortical bone. *J Biomed Mater Res A* 95(1):49-57
62. Shin SY, Park HN, Kim KH, Lee MH, Choi YS, Park YJ, Lee YM, Ku Y, Rhyu IC, Han SB, Lee SJ, Chung CP (2005) Biological evaluation of chitosan nanofiber membrane for guided bone regeneration. *J Periodontol* 76(10):1778-84

63. Schiffman JD, Schauer CL (2007b) One-step electrospinning of cross-linked chitosan fibers. *Biomacromolecules* 8(9):2665-7
64. Schiffman JD, Schauer CL (2007a) Cross-linking chitosan nanofibers. *Biomacromolecules* 8(2):594-601
65. Golub LM, Goodson JM, Lee HM, Vidal AM, McNamara DC, Ramamurthy NS (1985) Tetracyclines inhibit tissue collagenases. Effects of ingested low-dose and local delivery systems. *J periodontol* 56(11 suppl):93-7
66. Rifkin BR, Vernillo AT, Golub LM (1993) Blocking periodontal disease progression by inhibiting tissue-destructive enzymes: a potential therapeutic role for tetracyclines and their chemically modified analogues. *J periodontol* 64(8 suppl):819-27
67. Emerton K, Drapeau S, Pasad H, Rohrer M, Roffe P, Hoopper K, Schoolfield J, Jones A, Cochran D (2011) Regeneration of periodontal tissues in non-human primates with rhGDF-5 and beta-tricalcium phosphate. *J Dent Res* 90(12):1416-21